



Hazard and Impact Knowledge for Europe

## Deliverable 3.3

# Final case study report on subsidence assessment techniques, Po Basin area, Italy

### Authors and affiliation:

Valerio Comerci (ISPRA)  
Michele Morelli (ARPA Piemonte)  
Chiara D'Ambrogi (ISPRA)  
Pio Di Manna (ISPRA)  
Luca Mallen (ARPA Piemonte)  
Gabriele Nicolò (ARPA Piemonte)

E-mail of lead author:

[valerio.comerci@isprambiente.it](mailto:valerio.comerci@isprambiente.it)

Version: 2021.10.14

This report is part of a project that has received funding by the European Union's Horizon 2020 research and innovation programme under grant agreement number 731166. Scientific work is co-funded by the Geological Surveys and national funds allocated for science within the period 2018-2021.



Deliverable Data		
<b>Deliverable number</b>	D3.3	
<b>Dissemination level</b>	General Public	
<b>Deliverable name</b>	Final case study report on subsidence assessment techniques, Po Basin area, Italy	
<b>Work package</b>	WP3, Hazard and Impacts Method Development	
<b>WP Lead /Deliverable beneficiary</b>	GEUS/ISPRA	
Deliverable status		
<b>Submitted (Author(s))</b>	07/07/2021	V. Comerci, M. Morelli, C. D'Ambrogi, P. Di Manna, L. Mallen and G. Nicolò
<b>Reviewed/Verified(WP leader)</b>	04/10/2021	T. Larsen (GEUS)
<b>Approved (Project leader)</b>	14/10/2021	Hans Doornenbal [TNO]



## TABLE OF CONTENTS

1	INTRODUCTION .....	3
1.1	Document Background and Scope .....	3
1.2	Abbreviations.....	3
1.3	HIKE WP3 contributors.....	4
2	HIKE WP3 CASE STUDY AMBITIONS AND EXPECTED IMPACTS.....	5
2.1	The case study concept .....	5
2.2	Summary of case study technologies.....	5
3	OBJECTIVES OF THE CASE STUDIES ON THE PO PLAIN (ITALY).....	6
4	SUMMARY/ABSTRACT.....	7
5	KEYWORDS.....	9
7	CASE STUDY ENERGY EXPLOITATION/STORAGE .....	17
8	METHODOLOGY/ ANALYSIS/ UNCERTAINTY EVALUATION/ DISCUSSION .....	18
	<i>COMPARISON WITH THE GEOLOGICAL DATA AND SEISMIC LINE INTERPRETATION</i> .....	33
9	POTENTIAL IMPACT .....	43
10	IMPORTANCE OF FAULT DATABASE TO THE METHODOLOGIES APPLIED IN THE PO PLAIN CASE STUDIES .....	44
11	CROSS-CUTTING RELATIONS BETWEEN CASE STUDIES.....	46
11.1	Cross-cutting: uncertainty estimates.....	46
11.2	Cross-cutting: Scientific basis for guidelines to authorities.....	47
12	BEST PRACTICE WITHIN THE FIELD OF GROUND DEFORMATION ASSESSMENT METHODOLOGIES .....	48
13	RELEVANCE OF THIS STUDY TO THE NEW GREEN DEAL AND PROPOSED FUTURE STUDIES.....	52
14	REFERENCES .....	53
15	SUPPLEMENTARY MATERIAL.....	63



# 1 INTRODUCTION

## 1.1 Document Background and Scope

This document presents the HIKE WP3 Final report. The document contains a description of the case study methodologies, case study settings, and work in progress. In addition to each individual contribution of WP3, this document also focuses on expected interaction with the HIKE European Fault database (FDB) and cross cutting relations between case studies. It is the objective to give an in-depth description of the individual case studies, report on how the work is evolving, and show the way forward for the future work.

## 1.2 Abbreviations

HIKE	= Project "Hazards and Impacts Knowledge Europe"
GIP	= Project "Geo-Information Platform"
EGS	= EuroGeoSurveys organization
GEEG	= Geo-Energy Expert Group (EGS)
EOEG	= Earth Observation Expert Group (EGS)
MREG	= Mineral Resources Expert Group (EGS)
WREG	= Water Resources Expert Group (EGS)
SIEG	= Spatial Information Expert Group (EGS)
EC	= European Commission
MS	= Member States
NGO	= Non-Governmental Organization
EGDI	= European Geo Data Information Platform
DMP	= Data Management Plan
PIP	= Project Implementation Plan
PMB	= Project Management Board (project lead + work package leads)
PA	= Project Assembly
PL	= Project Lead
WPL	= Work Package Lead
TL	= Task Lead
CDE	= Communication, Dissemination and Exploitation (plan)
FDB	= Fault database
HIDB	= Hazard and Impacts database
SHARE	= Project "Seismic Hazards Research Europe"
EPOS	= Project "European Plate Observing System"
MICA	= Project "Mineral Intelligence Capacity Analysis"
DOI	= Digital Object Identifier
GSO	= Geological Survey Organization
INSPIRE	= Infrastructure for Spatial Information in Europe
GEOSCI ML	= data model and data transfer standard for geological data
SI	= International System of Units



### 1.3 HIKE WP3 contributors

#	Participant Legal Name	Institution	Country
1	Nederlandse Organisatie voor Toegepast Natuurwetenschappelijk Onderzoek TNO	TNO (coordinator)	Netherlands
2	Albanian Geological Survey	AGS	Albania
3	Geologische Bundesanstalt	GBA	Austria
4	Royal Belgian Institute of Natural Sciences – Geological Survey of Belgium	RBINS-GSB	Belgium
5	Geological Survey of Denmark and Greenland	GEUS	Denmark
6	Bureau de Recherches Géologiques et Minières	BRGM	France
7	Bundesanstalt für Geowissenschaften und Rohstoffe	BGR	Germany
8	Landesamt für Bergbau, Geologie und Rohstoffe Brandenburg	LBGR	Germany
9	Landesamt für Geologie und Bergwesen Sachsen-Anhalt	LAGB	Germany
10	Bayerisches Landesamt für Umwelt	LfU	Germany
11	Islenskar orkurannsoknir - Iceland GeoSurvey	ISOR	Iceland
12	Istituto Superiore per la Protezione e la Ricerca Ambientale	ISPRA	Italy
13	Servizio Geologico, Sismico e dei Suoli della Regione Emilia-Romagna	SGSS	Italy
14	Agenzia Regionale per la Protezione Ambientale del Piemonte	ARPAP	Italy
15	Lietuvos Geologijos Tarnyba prie Aplinkos Ministerijos	LGT	Lithuania
16	Państwowy Instytut Geologiczny – Państwowy Instytut Badawczy	PIG-PIB	Poland
17	Laboratório Nacional de Energia e Geologia	LNEG	Portugal
18	Geološki zavod Slovenije	GeoZS	Slovenia
19	State Research and Development Enterprise State Information Geological Fund of Ukraine	GEOINFORM	Ukraine



## **2 HIKE WP3 CASE STUDY AMBITIONS AND EXPECTED IMPACTS**

### **2.1 The case study concept**

HIKE WP3 developed and tested novel methodologies building on top of results from previous projects and research. The work dealt with advanced current state-of-the-art knowledge across different energy exploitation scenarios and various geological settings. The final goal is to improve hazard and impact assessments and provide the basis for better standardization of these evaluations across Europe. With the joint development of methods, workflows and datasets an intensified research collaboration and improved transfer of knowledge has been established.

Different types of energy exploitation of the subsurface give rise to different challenges. These include, but are not limited to: induced seismicity, induced subsidence, as well as reservoir sealing and leakage. The processes are to a varying degree relevant for both energy extraction and subsurface storage. A common theme for these hazards is the importance of faults. Faults can guide subsurface motion as well as provide pathways for leakage. Furthermore, faults can be activated due to changes in external conditions such as pressure changes and lubrication by liquids.

Based on the participating partners' expertise four case studies have been formulated to cover as broad a range of methodologies as possible. In all case studies the relevance of the fault database established in WP2 has been explored. Furthermore, cross-cutting relations between individual case studies have been identified. The outcome of the case studies will be made publicly available through the share point in WP4 and through relevant meetings and publications.

### **2.2 Summary of case study technologies**

- Advanced localization of seismic events in Europe; Denmark, Netherlands and Iceland case studies
- Evaluation of methodologies for the assessment of ground deformation; Po Basin, Italy case studies
- Development and application of novel methods for reservoir sealing assessment; Poland case study
- Assessment of seismicity and safety in storage, Lacq Rousse, France case study



### **3 OBJECTIVES OF THE CASE STUDIES ON THE PO PLAIN (ITALY)**

In this report we present two case studies: Po Plain 1, localized in Emilia-Romagna region, and Po Plain 2 in Piemonte region. Both the case studies show methodologies relevant for the assessment of induced hazards and impacts that are related to the exploitation of subsurface resources, contributing to the overall HIKE objectives.

#### **Case study Po Plain 1**

The objectives of the case study Po plain 1 are twofold: 1) highlight the uncertainties in the evaluation of ground motion and indicate current guidelines and best practices at national and European levels; 2) show the importance of having a high-detail 3D geological model (i.e. chronostratigraphy and lithology of Pleistocene-Holocene sedimentary bodies and and faults) to better estimate the natural component of the subsidence.

Therefore, in this report we present 1) a case of controversial evaluation of land subsidence in a territory located a few kilometers south of the current Po river delta (Emilia-Romagna region), the “Guidelines for monitoring seismicity, ground deformation and pore pressure in subsurface industrial activities”, issued by the Italian Ministry of Economic Development, and the requirements established by the European Environment Agency for the GNSS stations to be used for the validation of the InSAR data of the European Ground Motion Service (EGMS); 2) a methodological approach, applied to a highly detailed 3D geological model of an area in the central Po plain (Lombardia region), aimed at defining the long-term natural component of subsidence, considering the role of compaction and tectonic activity.

#### **Case Study Po Plain 2**

The objective of the case study of Po Plain 2 was evaluation of methodology for induced surface displacements. In particular, we applied the PS-InSAR technique over Piemonte region (western Po Plain) as a tool to assess the present-day crustal mobility that could correlate with the active faults distribution and/or tectonic mobility.

PS-InSAR data have been recently used to analyse the mobility of well-known tectonic structures or for monitoring landslides on mountain slopes (Allievi et al., 2003; Antonello et al., 2004; Bürgmann et al., 2006; Colesanti et al., 2000, 2003a, 2003b; Farina et al., 2006; Ferretti et al., 2005; Funning et al., 2007; Herrera et al., 2009; Hilley et al., 2004; Massironi et al., 2009, Notti et al., 2014, Ciampalini et al., 2016). Conversely, PS-InSAR data are less frequently used for the analysis of tectonic mobility at regional scale, in order to improve seismotectonic models by detection of unknown tectonic structures, active faults or to asses local crustal mobility trends (Morelli et al., 2008, 2011, Perrone et al., 2013). Such approach has been tempted in the present project, where two distinct regional geological sectors, each one characterized by different uplift and/or erosion rates and tectonic regime, have been chosen to detect active faults.



## 4 SUMMARY/ABSTRACT

### Case study Po Plain 1

In the last years, the advanced synthetic aperture radar (SAR) interferometry (InSAR) has proven its effectiveness in the assessment of ground motion with millimetric accuracy. Its integrated use with traditional (in-situ) topographic height determination techniques, such as geometric leveling and Global Navigation Satellite System (GNSS), is consolidated in underground fluids extraction areas for detecting and monitoring land subsidence. Nevertheless, the lack of a specific standardized methodology does not allow for evaluating different results obtained from different types of analysis. Starting from the description of two independent estimations of land subsidence in the Agosta (Comacchio, Italy) area, where an environmental impact assessment procedure was carried out following a request for gas exploitation, this report points out the need for a standardized methodology, focused on the in-situ calibration of InSAR data. This last purpose requires an adequately dense and homogeneous reference GNSS network. The in-progress initiatives, at the European and national level, aiming at providing a Copernicus Ground Motion service could offer the opportunity to structure a reliable and dedicated GNSS network, starting from the large number of stations run by different institutions already existing in Italy.

A methodology for the assessment of the tectonic contribution to subsidence is also provided, showing the need for well constrained chronostratigraphic information to be added to the tectonic data. Therefore, the complementation of 3D faults included in the Fault Database with detailed chronostratigraphic data would allow further and wider application of the up to now stored information.

### Case Study Po Plain 2

In order to analyse the present crustal mobility and neotectonics of NW Italy, namely the so-called “Alps-Appennines interference zone”, spatial statistics (Hot Spot and geostatistical analysis) of PS-InSAR (Permanent Scatterers Interferometric Synthetic Aperture Radar) data has been done, with the aim to shed lights on the relation between fault systems and seismic activity of the region.

This analysis allowed to define a number of kinematically homogenous areas, represented in some Iso-Kinematic maps (IKM), where the homogenous areas are inferred to represent sectors characterized by relative ground movements (uplift or sinking) and maybe different tectonic regime. These movements should occur mainly along the boundaries (IKB) of the IKM areas. The distribution of the IKB, which may thus correspond to regional faults or tectonic contacts, have been compared with the surface data of the Piemonte Geological Map at 1:250,000 scale, with subsurface stratigraphic and tectonic data (interpreted on seismic lines provided by ENI SpA in the frame of the “HotLime GeoEra” project, funded by the European Union, Horizon 2020) and with the available seismological and GPS data.

The IKM seem to indicate differential uplifting ratios between the inner Cottian Alps and the Western Po Plain, separated by some N-S major faults: (e.g., the Col del Lis-Trana and the Cavour tectonic lineaments), as well as between the western termination of the N-verging Padane Thrust Front (Monferrato Front) and the Padane plain. Furthermore, the Villalvernia-Varzi Line and Scrivia fault seem to constrain the distribution of the IKM



---

and IKB, while further investigations are required for the interpretation of the SW Alps internal boundary and the adjoining Langhe sedimentary domain.

The ground motion tendency suggested by IKM seems to be in overall agreement with the different geological and geophysical datasets. This correspondence suggests a current tectonic mobility and the differential uplift of the sectors analysed mostly driven by the activity of above major faults. Therefore on the basis of these good agreements, this methodology could also be used to associate a “weight” about the tectonic activity of faults as future expansions of the HIKE fault database.



## 5 KEYWORDS

Ground deformation / deformations; subsidence; human health and safety consequence; people / social; subsurface management (category) economic; environmental impact/ environmental impact of energy/ environmental risk / environmental monitoring; site of pumping stations and/or pipelines; conventional energy / natural gas extraction/ reservoir gas/ oil, gas and chemicals pumping station/ oil, gas and chemicals plant; hydrocarbons (oil and gas) / oil, gas and chemicals pumping station/ oil, gas and chemicals plant; subsurface exploration / underground mining; CO2 storage; natural hazard; earthquake / tremor; analytical method; monitoring; geophysics /geophysical survey / Applied Geophysics (category); data acquisition; earth surface setting / geology; tectonics /tectonic process / tectonic and structural features/ tectonically defined setting; structural geology elements / category Structural Geology; Geochronology, Stratigraphy; lithostratigraphic unit; chronostratigraphic units.



## 6 GEOLOGICAL SETTING

### 6.1 Case study Po Plain 1

The investigated area, located in the southeastern part of the Po Plain (Figure 6.1.1), constitutes a portion of the Plio-Quaternary foreland basin of the Apennine chain, thrust northeast onto the Adriatic plate (Carminati et al., 2003a; Fantoni & Franciosi, 2010). The lower portion of Quaternary sedimentary succession of the Po River and Adriatic coast that fills this basin is structured in a series of parallel-oriented folds and thrusts with an orientation about NW–SE and reaches the maximum thickness of about 2000 m (Pieri & Groppi, 1981; Cassano et al., 1986). These thrust-related ridges, known as Emilia and Ferrara Folds (Pieri & Groppi, 1981), are approximately in concurrence of the present Po River course and represent the outermost Apennine fronts (Martelli et al., 2017)]. The Agosta anticline, part of the Ferrara Folds, due to subsidence both tectonic and by consolidation, is buried under Pleistocene and Holocene sediments; the only outstanding morphologies in the area correspond to paleo-channels, dune belts, and artificial banks bordering watercourses or reclaimed areas (Bondesan, 1982; Bondesan, 1990). Before the massive reclamation works carried out starting from 1873 and then, more intensely, between the years 1920 and 1960, almost half of the territory of Ferrara was occupied by watercourses, swamps, and marshes. The topographic surface currently ranges between -2 and +4 m above the sea level and a large part of it is occupied by the lagoon of the Comacchio valley (Figure 6.1.2).

The upper part of the Quaternary succession shows the alternating of clayey and silty alluvial (diffused palaeo-channels) deposits with sandy littoral (dune bars) and deltaic deposits (Figure 6.1.3). The surficial stratigraphy is generally composed, from top to bottom, by: half a meter of soil, 2–5 m of dark peat clay deposits, typical of fluvial-lacustrine facies with abundant shell remains, sandy deposits with peat levels and shell levels down to the depth of 12 m, compacted silty clay down to 16 m, and then silty sand deposits reaching the depth of 20 m.

The deviated well Agosta1 (2253 m deep, corresponding to -1989.7 m a.s.l.), had the first 1000 m drilled into Pleistocene sandy deposits with silt and clay intercalations (Emiliano-Romagnolo Supersynthem and other Quaternary deposits) and then the Pliocene turbiditic dominantly sandy levels of the Porto Garibaldi and Porto Corsini Formations, where two sandy layers resulted mineralized with gas (Figure 6.1.4).

About 8 km southeast of the Agosta field, the important Dosso degli Angeli gas field is located (Figure 6.1.1). The two reservoirs, placed at different depths, are considered hydraulically separate.

Through 32 abstraction wells deep from 2900 to 3800 m, Dosso degli Angeli has produced 32 billion Sm<sup>3</sup> of gas (94% of recoverable resources) in 1971–2004 (Simeoni et al., 2017) and, after an interruption of several years due to groundwater inflow, has resumed production in 2011 with 2027 as target closing date. In the 1970–1999 period, a subsidence up to 20 mm/yr was measured above the Dosso degli Angeli field (Bitelli et al., 2000) triggering the concern of the local communities. Since then, a decay of the lowering has been observed that is currently noticeably reduced. Despite appearing to be very modest in relation to the ongoing production, the effects of lowering induced by the Dosso field affect also the area of Agosta, based on modelling (Eni, 2015; Simeoni et al., 2017). Further south, closer to Ravenna, there are several gas reservoirs inducing local subsidence; however, their cones of influence do not reach the study area (Fiaschi et al., 2016).

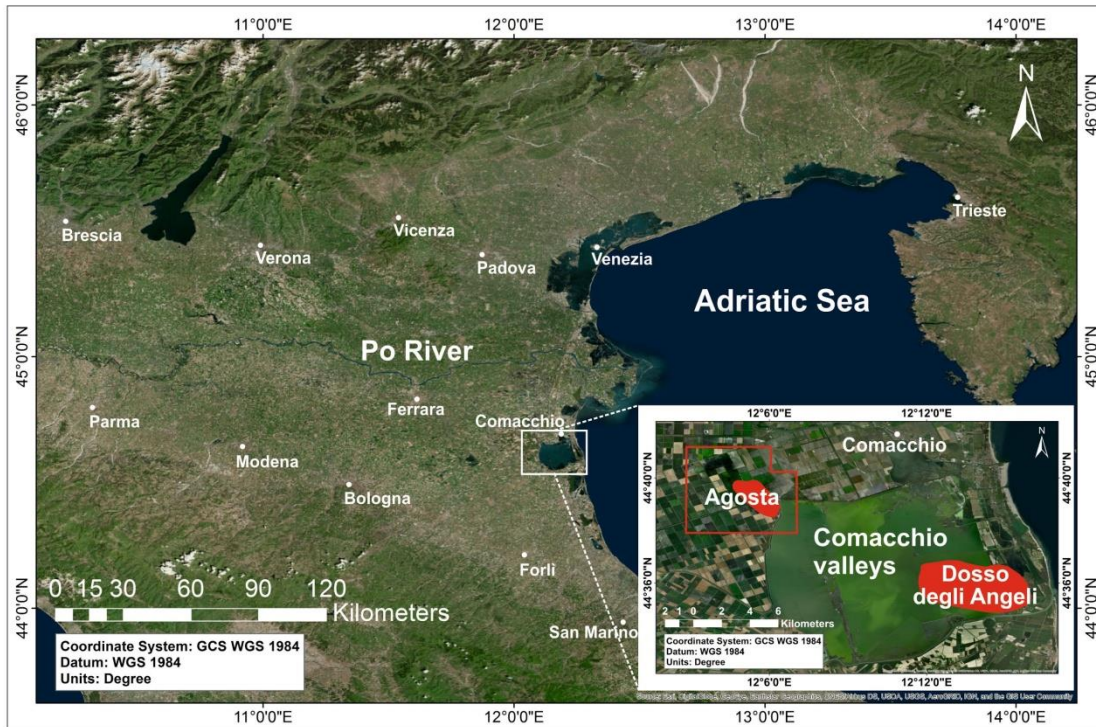


Figure 6.1.1: Location of the study area. The red empty polygon inside the zoom box represents the area of the Agosta1 concession while the red areas represent the surface projection of the Agosta and Dosso degli Angeli gas fields. Modified after (Eni, 2015). Base map source: Esri.



Figure 6.1.2: View of the Comacchio Valleys. Photo: N. Spadoni (ambiente.regione.emilia-romagna.it)

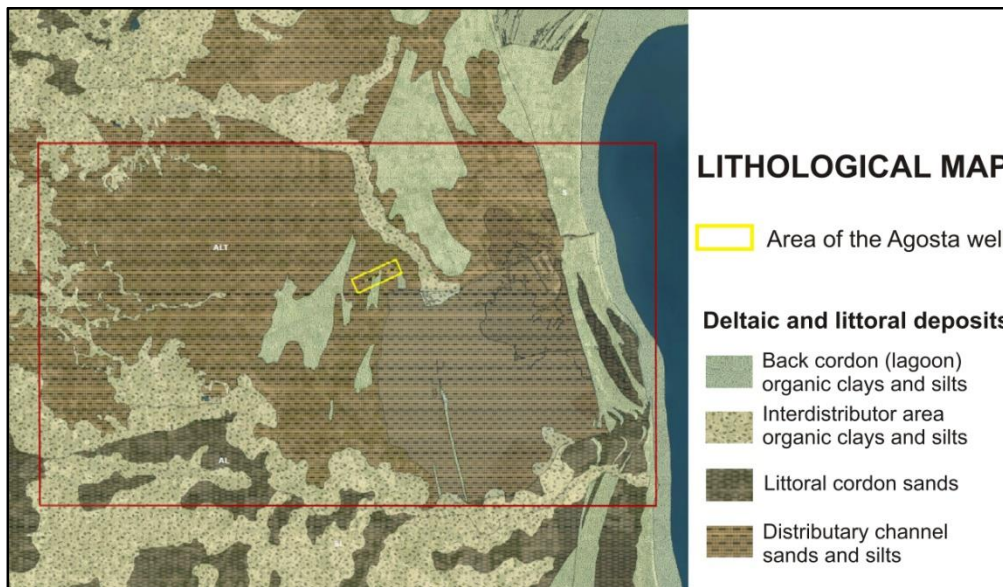


Figure 6.1.3: Extract of the Lithological map of Emilia-Romagna Region. Modified after Eni (2015).

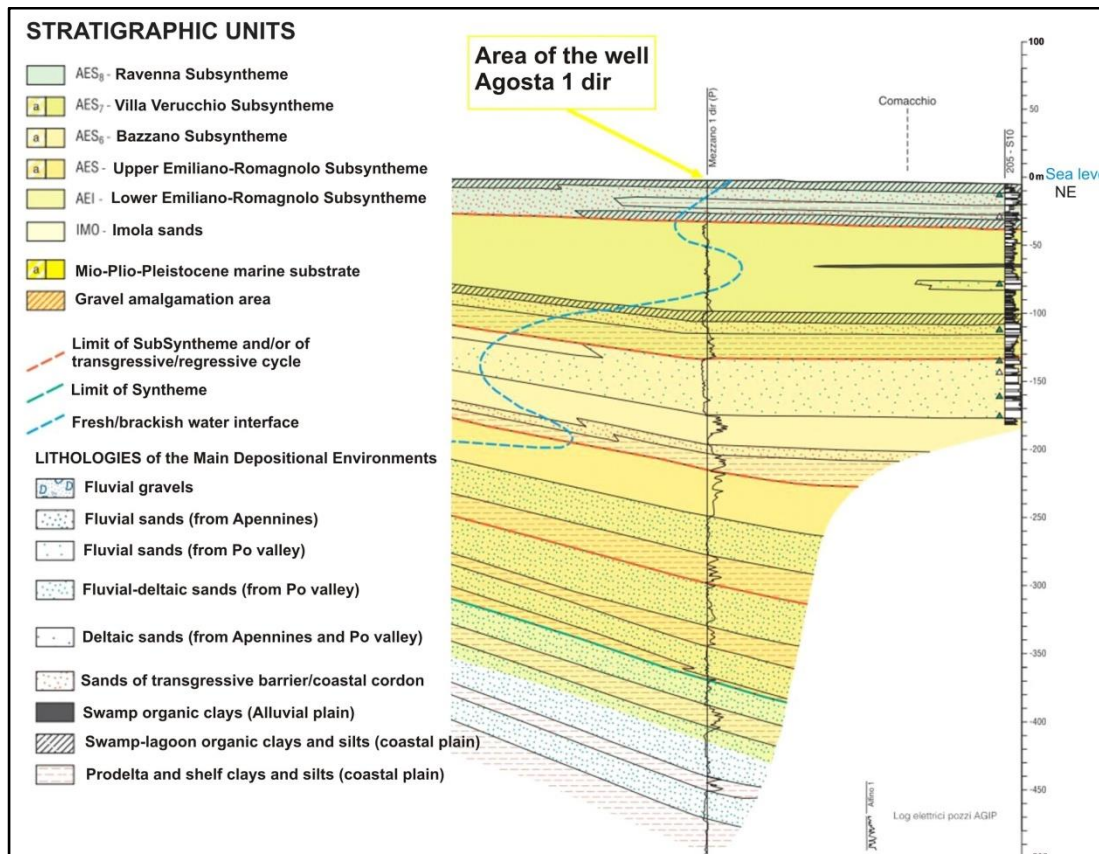


Figure 6.1.4: First 500m of the stratigraphy of the Well Agosta, 2,253 m deep (-1,989.7 m a.s.l.) Modified after Eni (2016b).



## 6.2 Case study Po Plain 2

Two distinct regional geological sectors located on the western part of the Po Plain have been chosen to detect active faults or/and to assess local crustal mobility trends. **Sector 1** encompasses the westernmost Po Plain between Turin Hill (TH) and the inner border of the Italian (Cottian) Western Alps, while **Sector 2** comprehends the junction zone between the Po Plain, the northern Apennines and the Ligurian Alps (Figure 6.2.1).

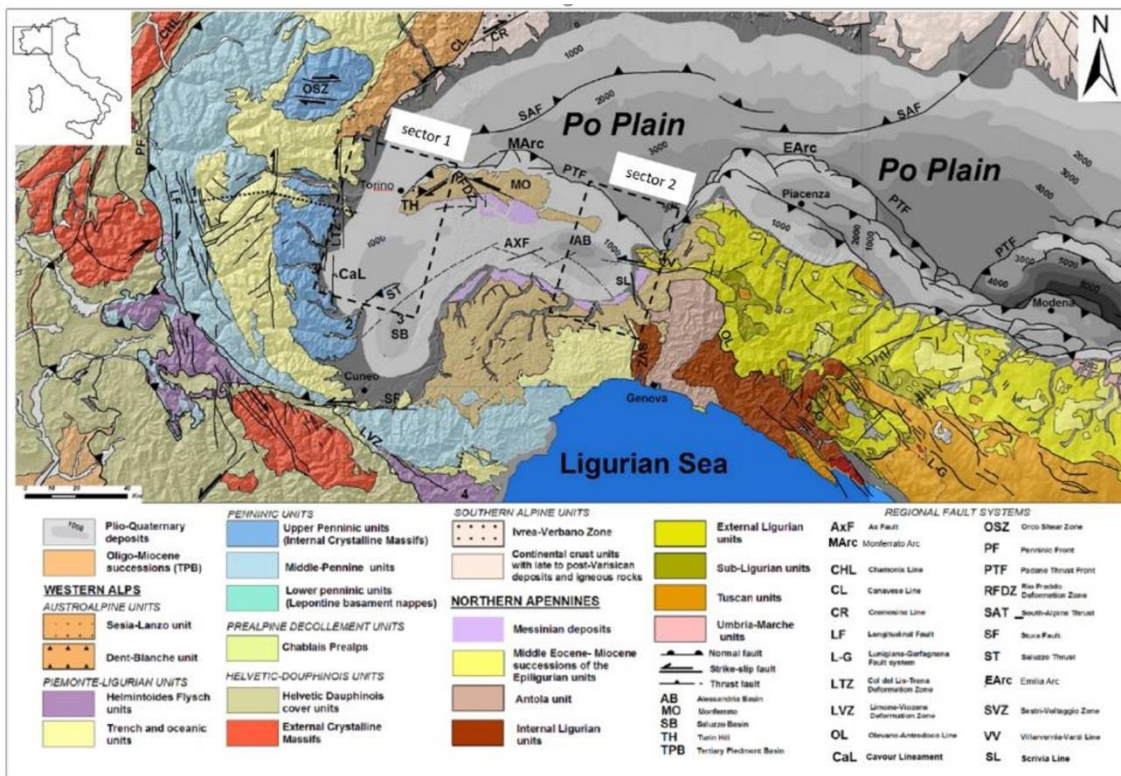


Figure 6.2.1. Tectonic sketch map of the north-western Italy (after Bigi et al., 1990; Dela Pierre et al., 2003; Festa et al., 2009; Gelati et al., 2010; Perrone et al., 2011). The black dashed square indicates the sectors analysed.

In Sector 1 and Sectors 2 the Quaternary deposits of the Western Po Plain mask at surface the tectonic junction area between the metamorphic units of the Western Alps, the Northern Apennines tectonic belt, the Southern Alps sedimentary successions resting on the Adria crust, some detached slices of non-metamorphic Ligurian units and the Oligocene-to-Pliocene succession of the inner Alpine synorogenic basins. The synorogenic basins are subdivided into four units: the north-Padane Oligocene–Miocene basin (Gonfolite Basin), the south-Padane Late Eocene-to-Late Miocene basin (“Tertiary Piemonte Basin” TPB), and the Plio-Pleistocene Savigliano the Alessandria Pliocene-Quaternary basins and Western Po Basin (Figure 6.2.1). The Gonfolite Basin, representing the foredeep of the South-Alpine thrust front, formed during the Oligocene (Gelati et al., 1988, Di Giulio et al., 2001), while the TPB developed in Oligocene-Miocene times as a complex sedimentary realm within which some partially independent domains (corresponding to Monferrato, Turin Hill, Langhe, Alto Monferrato and Borbera-Grue) can



be recognized (Gelati and Gnaccolini, 1988; Piana et al., 2000; Dela Pierre et al., 2003; Rossi et al., 2009) (Figure 6.2.1).

**Sector 1** includes the easternmost part of the Cottian Alps and the subsurface western termination of the TH sedimentary succession, which is masked at surface by the fluvial deposits of the present Western Po Plain. The major tectonic structures of this sector are (from West to East): (i) the Col del Lis-Trana Deformation Zone (LTZ) and (ii) the western termination of the N-verging Padane Thrust Front (PTF - Monferrato-Torino Hill thrust front) and (iii) the NW-verging Saluzzo Thrust (ST) (Figure 6.2.1).

- The Col del Lis-Trana Deformation Zone (LTZ in Figure 6.2.1) corresponds to an N–S, sub-vertical composite structure. Seismic and geological data suggest that LTZ should extend southwards along the inner Alpine border, beneath the Plio-Quaternary Po Plain deposits, reaching about 50 km in length. The LTZ acted as a dextral transpressive brittle–ductile shear zone and later, until Quaternary time, as a normal fault (Perrone et al., 2010, 2011a).
- The Monferrato-Torino Hill thrust front is a south-southeast-dipping surface, sealed by Late Pliocene to Pleistocene sediments, which marks the northern subsurface boundary of the Ligurian units and their overlying Torino Hill and Monferrato Oligocene-Miocene successions, and separates them from the Tertiary and Mesozoic sediments resting on the subsurface Adria basement. The PTF is mostly a blind thrust whose vertical projection at surface roughly corresponds to the geomorphologic southern boundary of the Po Plain (Amorosi et al., 1996; Boccaletti et al., 2011, Michetti et al., 2012). A complex rearrangement of fluvial drainage during the Mid-Pleistocene to Holocene that included the combining and diverting of major rivers (Carraro, 1976; Forno 1982; Dela Pierre et al. 2003) testifies to the important recent tectonic activity of PTF. Furthermore, topographic levelling (Arca and Beretta 1985) and recent GPS observations (Caporali et al. 2003, Devoti et al. 2011) have shown an uplift and shortening of a few mm/yr. along and across the PTF.
- The Saluzzo Thrust (ST) is a NE-SW striking thrust fault which was active from the Late Tortonian to the Lower Pleistocene (Ghielmi et al., 2002; Vigna et al., 2010) inducing some hundred-meters of vertical offset of the BTP and Pliocene successions, together with a NW-ward tectonic transport. The ST caused the partial differentiation of the Pliocene sedimentary basin placed south of the Torino Hill, separating it into two depocenters, the Moretta sub-basin to the West and the Fossano sub-basin to the East (Ghelmi et al., 2019).

Sector 1 is subjected to moderate differential uplift, as observed by GPS data (Devoti et al., 2011) and by low magnitude instrumental seismicity ( $ML < 5$ ) despite the fact that historically, earthquakes that have struck this area have reached up to a moderate magnitude (seismic event of April 2, 1808,  $M_s = 5.5$ ; Boschi et al., 2000). Seismicity is mostly concentrated along a longitudinal band, known as the Piedmont seismic arc, roughly sub-parallel to the inner border of the Western Alps. The hypocentres are relatively shallow inside the Alps, usually being confined within the first 15–20 km of crust. By contrast, in the Western Po Plain, the seismicity is distributed within the entire crust, reaching a depth of 40–50 km (Eva et al., 1997; Eva and Solarino, 1998). Focal mechanisms (Béthoux et al., 2007; Delacou et al., 2004; Eva and Solarino, 1998) indicate a contrasting stress regime in the inner Western Alps. Transcurrent and extensional mechanisms, with steep P axes and sub-horizontal roughly E–W trending T axes, largely occur in the Western Alps. Compressive and transpressive solutions, with



sub-horizontal roughly E–W trending P axes, instead occur in the westernmost Po Plain. The seismic activity of this area could be related to current tectonic slip-on N–S regional faults along the inner border of the Western Alps (Perrone et al., 2010, 2011a), as seismological and tectonic data show consistent geometry and kinematics. This suggests that the dextral transtensive regime in the Western Alps is still ongoing (Delacou et al., 2004, 2008; Perrone et al., 2010, 2011b; Sue et al., 2007; Sue and Tricart, 2003).

By contrast, in the westernmost Po Plain, focal mechanisms indicate that tectonic contraction is still ongoing, although the relations between faults and seismicity are poorly understood. Béthoux et al. (2007) hypothesized, based on seismic and magnetic interpretations, that the physical limit between these different stress regimes is represented by the southern prolongation of the Insubric Fault and associated very high-density rock bodies at depth.

More recent seismotectonic interpretations (Delacou et al., 2004, 2008; Perrone et al., 2010, 2011b) have shown that these data fit with a model that postulates transtensive deformation inside the Alpine chain, due to the coexistence of gravitational body forces and transcurrent movements, and transpressive deformation both in the more external (Jura chain) and internal (Western Po Plain) sectors. This implies that the convergence, associated with the anticlockwise rotation between the Adriatic and European plates, is still ongoing. Geodetic data show that the rotation pole of the Adria plate is located between the Western Po Plain and the French Alps (Anderson and Jackson, 1987; Calais et al., 2002; Ward, 1994).

**Sector 2** lies on the Padane Thrust Front (PTF) between the Monferrato thrust front and Emilia thrust front, the Villalvernia-Varzi Line (VVL) and Scrivia line (SL) represents one of the few seismic sectors of the Piedmont Region in NW Italy as shown by recent seismic events (INGV, 2007) that caused significant damage to local population and facilities (e.g., 4,6 MI event of Sant’Agata Fossili in Spring 2003; see INGV, 2007).

- Monferrato and Emilia thrust fronts are currently buried below the Pliocene–Quaternary marine and continental deposits infilling the Po Plain basin and are organized in the complex thrust fold systems. Seismicity is not evenly distributed, however, increases from west to east, i.e. from Monferrato the Emilia.

The present-day activity of these two thrust fronts is characterized by compressional focal mechanisms (<http://www.bo.ingv.it/RCMT/searchRCMT.html>) in agreement with tectonic evidence.

- Villavernia – Varzi Fault Zone (VVL) is a E-striking and steeply dipping regional fault zone, separating External Ligurian Units and Epiligurian Units of the Northern Apennines, to the North, from Tertiary Piedmont Basin successions, to the South. It was active in early Oligocene – Miocene time span (Ghibaudo, et al., 1985, Mutti et al., 1995, Di Giulio & Galbiati, 1995; Felletti, 2002; Rossi et al., 2009; Mosca et al., 2010; Festa et al. 2015), playing a significant role in the westward-indentation of the Adria microplate with the Western Alpine belt (Castellarin, 1994; Laubscher et al., 1992). The VVL is a high-angle pre-Oligocene extensional fault reactivated as contractional or transpressive fault during the N-NE verging thrusting of Apennines Ligurian units (middle-late Rupelian, see Di Giulio and Galbiati (1995). The main activity of the VVL is considered to be Late Oligocene-Early Miocene in age and it is interpreted as an outstanding sinistral transfer fault zone (Laubscher et al. 1992; Schumacher and Laubscher, 1996; Festa et al. 2015)



at the southern margin of the Adriatic indenter (Laubscher, 1988; Laubscher, 1991), parallel to the Insubric Line and with an opposite kinematics. In this framework the VVL was dissected by late Serravallian-Tortonian transtensional faults and post-Messinian thrusting, as the Adriatic indenter appears to have been inactivated in post-Miocene times (Schumacher and Laubscher, 1996). At present the VVL is characterized by a weak seismicity (Tomaselli et al. 1992, INGV, 2007).

- Scrvia Line (SL) is an N-S striking and steeply dipping regional fault zone (Gelati 1977) interpreted as an Oligocene–Miocene syn-sedimentary fault (Ghibaudo et al., 1985, Capponi et al., 2009). According to d’Atri et al. (2002) it could represent the prosecutions toward the North of Sestri-Voltaggio Line, a steeply dipping N-S striking, composite fault that juxtaposes Briançonnais units and high-pressure meta-ophiolites of Voltri Unit (Ligurian Alps) to the unmetamorphosed Antola flysch unit of the External Ligurian units (Northern Apennines) (Scholle, 1970; Elter and Pertusati, 1973; Sturani, 1973; Cortesogno et al., 1979, Cortesogno and Haccard 1984; Hoogerduijn Strating, 1991, Abbate and Sagri 1984; Ellero, 2000; Cerrina et al. 2002; Levi et al. 2006; Capponi et al., 2009). During the Late Oligocene the SL induced the uplift of the western sector respect to the eastern one, whilst during Burdigalian and early Langhian times it induced an opposite reactivation trend, which was sealed by Langhian sediments (Ghibaudo et al., 1985). Moreover, some Authors underline sinistral transcurrent movements on the main faults occurring along the tectonic lineament corresponding to the Scrvia River during the Pliocene time (Perotti, 1985; Fossati et al., 1988). Detailed morpho-tectonic studies, as well as analyses on fluvial dynamics and alluvial sediments distribution along the Scrvia river (or lineament) suggest a late Pleistocene-Holocene differential tectonic uplift and neotectonics activity along it (Boni et al., 1980, Meisina, 2003 Cortemiglia 1981a; ENEL 1981, Mandarino et al., 2015) with a progressive migration of the river direction from SE-NW to currently N-S.



---

## 7 CASE STUDY ENERGY EXPLOITATION/STORAGE

Underground gas storage in depleted hydrocarbon reservoirs is a strategic practice to cope with the growing energy demand and occurs in many places in Europe and worldwide.

The Po plain has historically been the site of hydrocarbons research and extraction. Moreover, several depleted hydrocarbon fields are used for gas storage. In particular, case study 1 analyses the effects on the surface of the exploitation of oil fields (see Figure 6.1.1). The described methodologies are in general useful for the assessment of ground motion induced by natural phenomena or anthropogenic activities like underground fluids extraction. The effectiveness of the satellite data (e.g. InSAR) is now well established for surface monitoring of underground mining or storage activities. In fact, it is considered in the national guidelines for monitoring seismicity, ground deformation, and pore pressure in subsurface industrial activities. Their combined use with detailed geological data, including those on faults, in particular 3D, allow us to build evolution models that are now essential for planning and monitoring of subsurface industrial activities.



## 8 METHODOLOGY/ ANALYSIS/ UNCERTAINTY EVALUATION/ DISCUSSION

### 8.1 Po Plain 1

The integrated use of advanced synthetic aperture radar interferometry (InSAR) with traditional (in-situ) topographic height determination techniques, such as GNSS, is consolidated in underground fluids extraction areas for detecting and monitoring land subsidence. Nevertheless, the lack of a specific standardized methodology does not allow for evaluating different results obtained from different types of analysis.

Here, it is presented a case of controversial evaluation of land subsidence in a territory located in the Po alluvial Plain (Figure 6.1.1), a few kilometers south of the current river delta in the Comacchio Valleys, a complex of brackish lagoons and wetlands close to the Adriatic Sea. Located in the municipal territory of Comacchio (province of Ferrara), the exploration well Agosta1, about 2000 m deep, discovered a gas reservoir. The oil and gas company Eni S.p.A. applied for permission to exploit the Agosta reservoir (the estimated lifetime of two production strings is 13 years), submitting its project to the evaluation of the Italian Ministry of the Environment (MATTM), which is in charge of the Environmental Impact Assessment (EIA). About 8 km southeast of the Agosta field, the important Dosso degli Angeli gas field is located (Figure 6.1.1). The two reservoirs, placed at different depths, are considered hydraulically separate. In the 1970–1999 period, a subsidence up to 20 mm/yr was measured above the Dosso degli Angeli field. Since then, a decay of the lowering has been observed that is currently noticeably reduced.

Based on modelling, the effects of lowering induced by the Dosso field affect also the area of Agosta.

Being the considered territory prone to land subsidence, the ground lowering induced by gas exploitation for the estimated duration of the concession was one of the impacts considered by MATTM in the EIA. In order to prepare its assessment, MATTM consulted, among others, the Emilia Romagna Region that, with the technical support of the Regional Environmental Agency (ARPAE), has been monitoring subsidence phenomena on the whole regional territory since 2002. The measurements of the current land subsidence carried out independently by ARPAE and by Eni show a slight difference of about 4–5 mm/yr. Such a difference, even if small in absolute, becomes relevant for the correct evaluation of the impact induced by the gas extraction activity, which generally lasts for decades. ARPAE based its assessment on PSInSAR and SqueeSAR results, while the later Eni only on SqueeSAR. The analyzed stacks of satellite SAR images were not exactly the same (Tables 8.1.1 and 8.1.2).

Satellite	Geometry	n. images	n. scatterers	Period
ERS 1-2	Asc	40	8,480	03/07/1992-01/01/2001
ERS 1-2	Desc	67	12,650	10/05/1992-13/12/2000
RSAT1	Asc	109	34,044	08/05/2003-16/12/2011
RSAT1	Desc	99	35,232	25/04/2003-27/12/2011

Table 8.1.1. Dataset of SAR data analyzed by Eni



Satellite	Geometry	n. images	n. scatterers	Period
ERS 1-2	Desc	65	14,249	10/05/1992-13/12/2000
Envisat	Desc	n.d.	34,816	04/2003-02/2006
Envisat	Asc	n.d	32,782	06/2003-03/2006
RSAT1	Asc	67	55,024	16/01/2006-30/04/2011

Table 8.1.2. Dataset of satellite SAR data analyzed by ARPAE

InSAR data lacks an absolute reference datum and are affected by low frequency velocity noise that can be removed by GNSS calibration. In order to calibrate the InSAR data with in-situ constraints, both ARPAE and Eni used Continuous Global Positioning System (CGPS) data, but belonging to different GNSS networks.

The differences in the two independent evaluation processes mean that the two estimates are not directly comparable. Even if not the only reason, the uncertainties on the estimation of the subsidence rate induced by gas exploitation were certainly among the motivations that led the region to give an unfavorable evaluation of the project.

ISPRA provided technical support to the MATTM committee in charge of the EIA in the evaluation of the studies carried out by Eni on the expected induced subsidence. The data here reported are published in the MATTM website <http://www.va.minambiente.it/en-GB/Oggetti/Info/1552>.

Eni simulated the expected subsidence both at Dosso degli Angeli and at Agosta from 1980 to 2060 by applying a finite-element elasto-plastic geomechanical model. Two separate fluid dynamic studies were performed for the two reservoirs. The results of the simulation were compared with the available control points represented by a GPS station (at Smarlacca, Ravenna province) above the Dosso degli Angeli field, two geometric levelling benchmarks, and five SqueeSAR scatterers.

The comparison between measured and computed data requires that the former are “cleaned” from subsidence components not attributable to gas extraction (in this case the Dosso field production). The subsidence non-attributable to gas extraction is composed of compaction and oxidation of surface sediments (rich in organic matter), water abstraction component, and a deep tectonic component. Acknowledging the high local variability and uncertainty about the amount of tectonic subsidence, Eni assumed, for the whole area under examination, an average subsidence component not attributable to gas extraction of -5 mm/yr, based on recently integrated analyses.

Eni analyzed InSAR data from 1992 to 2011 over an area extending from Ravenna to the Comacchio valleys. In particular, line of sight (LOS) SAR images in ascending (Asc) and descending (Desc) geometry (Table 8.1.1) processed with SqueeSAR technique and derived vertical velocity maps (Figure 8.1.1) were analyzed. ARPAE also carried out its own analysis (Table 8.1.2), over a slightly larger area. The 1992–2006 data were processed with the PSInSAR technique and the 2006–2011 data with the SqueeSAR technique.

Furthermore, ARPAE published the Regional vertical velocity maps for the following years: (a) 1970/93–1999, based on geometric levelling data; 1992–2000, based on PSInSAR data calibrated with levelling data (Figure 8.1.2a); (b) 2002–2006, based on



PSInSAR data calibrated with leveling data (Figure 8.1.2b); (c) 2006–2011, based on the SqueeSAR data, calibrated with 16 CGPS stations (Figure 8.1.2c).

With the aim of calibrating the satellite data with an in-situ constraint, Eni used a CGPS station, located at Smarlacca (in the province of Ravenna), above the Dosso field (Figure 8.1.3), controlled and certified by the Bologna University. The Smarlacca station, managed by Eni together with four other nearby stations, from 2002 until 2015 showed an average velocity of -6.48 mm/yr. Eni calibrated the 2003–2006 and the 2006–2011 InSAR data by adding them to the difference in velocities between the Smarlacca CGPS (-8.18 and -6.10 mm/yr) for the two time periods and the average velocities for the same periods of the backscatterers within 150 m from the CGPS. Moreover, Eni analyzed COSMOSkyMed (CSK) Asc and Desc SqueeSAR data for the period 2012 – 2015, calibrated with the Smarlacca CGPS and the results were validated with the Spinaroni CGPS (that in the period 2002–2015 showed a velocity of -7.58 mm/yr), located about 11 km South of Smarlacca. The SAR scatterers falling within a radius of 100 m from the Smarlacca CGPS have been used for calibration, their average velocity resulting -1.56 mm/yr. In order to calibrate with the velocity of the Smarlacca CGPS (-6.48 mm/yr) their velocity, the value of -4.92 has been added to them. Afterwards, the calibrated velocities of the scatterers falling within 100 m from the Spinaroni CGPS have been compared with the velocity of the Spinaroni CGPS, resulting in good agreement. Figure 8.1.4 shows the CSK calibrated vertical components.

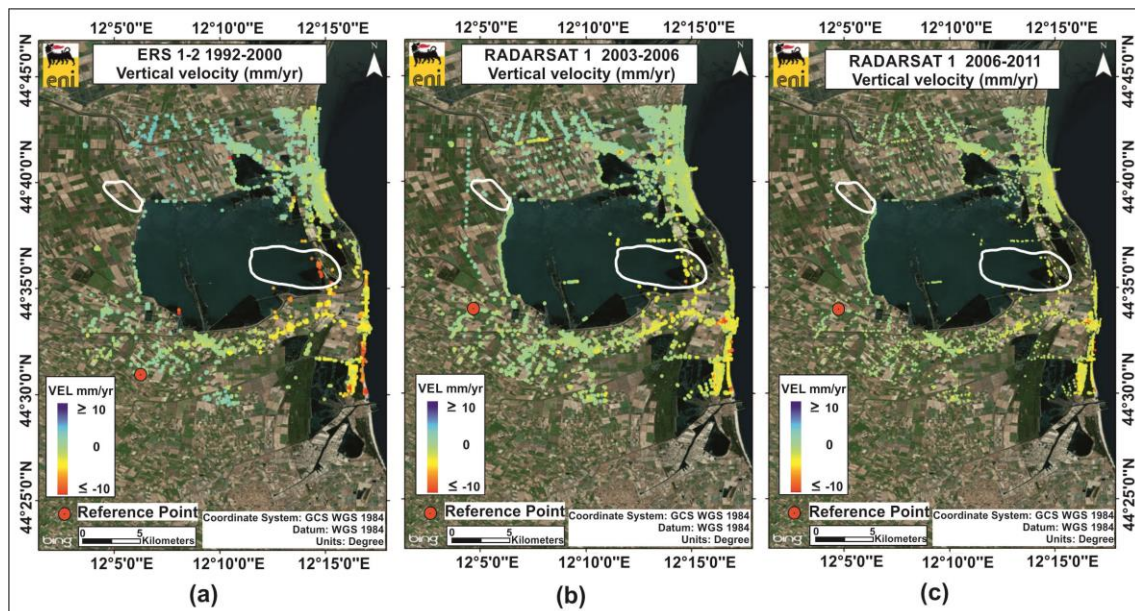


Figure 8.1.1: (a) Vertical average annual velocities of ERS 1-2 data (1992–2000); (b) Vertical average annual velocities of RSAT 1 data (2003–2006); (c) Vertical average annual velocities of RSAT 1 data (2006–2011). White polygons represent the surface projection of the Agosta and Dosso degli Angeli fields.

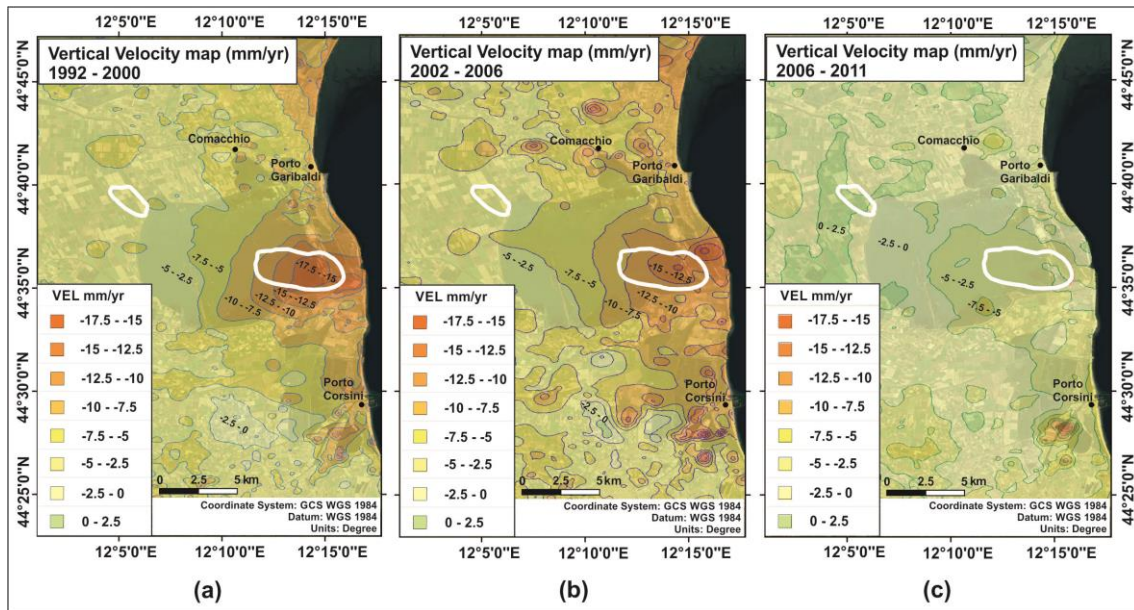


Figure 8.1.2: Vertical velocity maps interpolated from InSAR data and calibrated by ARPAE (extracted from ARPAE environmental geospatial website: <https://arpae.it/cartografia/>), related to the time periods: (a) 1992–2000; (b) 2002–2006; (c) 2006–2011. White polygons represent the surface projection of the Agosta and Dosso degli Angeli.

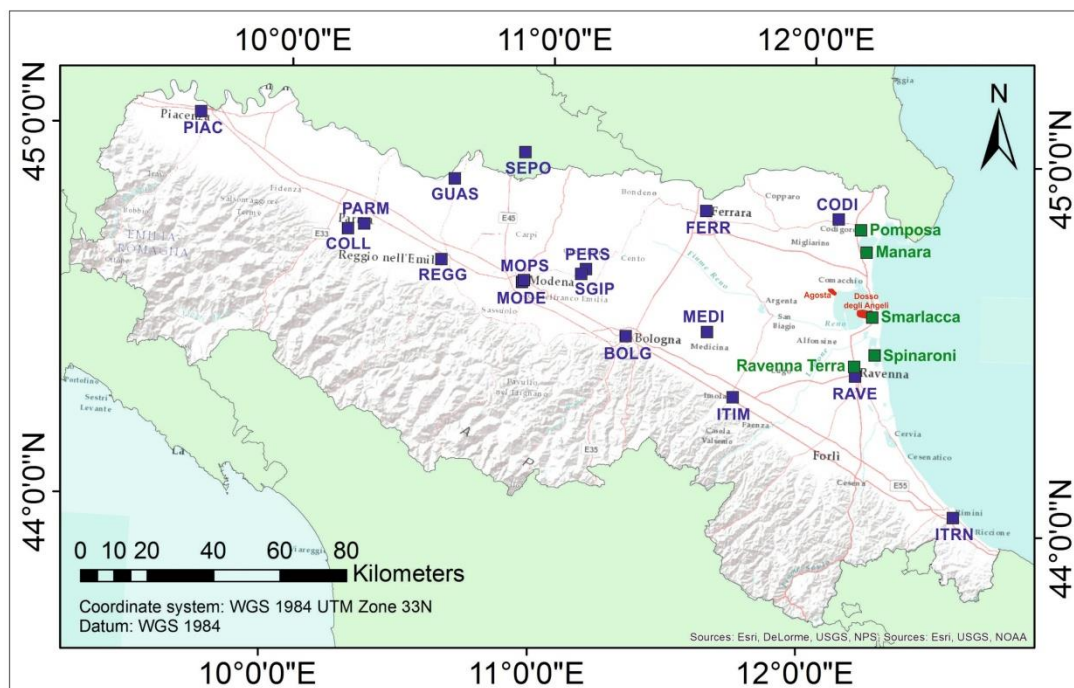


Figure 8.1.3: Location of the five CGPS stations (in green) closest to Agosta managed by Eni S.p.A. and of the 17 CGPS stations (in blue) managed by the Emilia Romagna Region and belonging to three different geodetic infrastructures. ARPAE used them to define the datum and to calibrate the 2006–2011 SqueeSAR (RADARSAT) data.

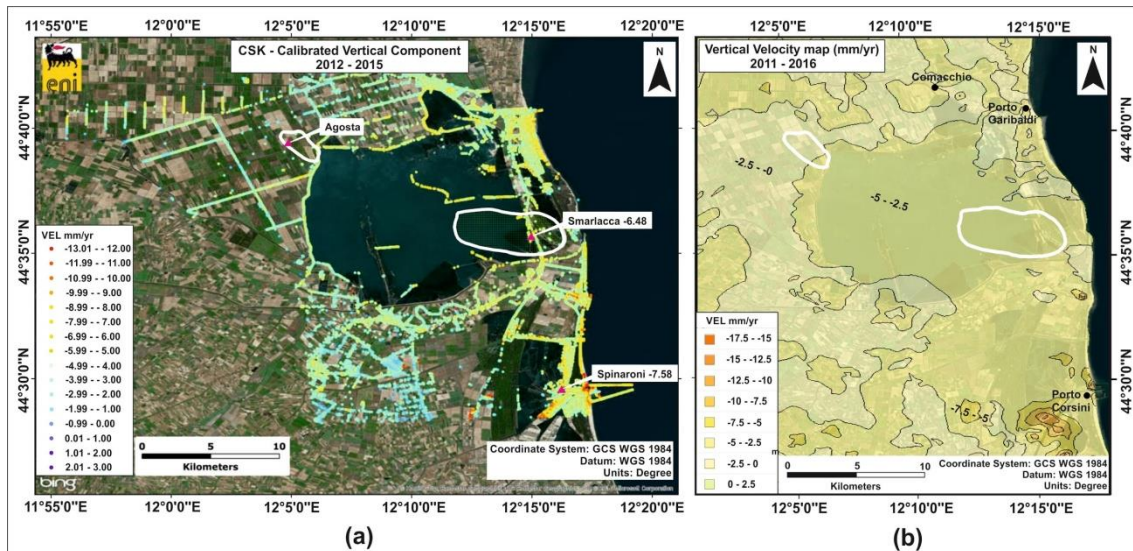


Figure 8.1.4: (a) COSMO-SkyMed (CSK) vertical velocities calibrated with the Smarlacca CGPS and validated with the Spinaroni CGPS by Eni. The Smarlacca and Spinaroni CGPS velocities (in mm/yr) are also indicated; (b) 2011–2016 vertical velocity map interpolated from InSAR data and calibrated by ARPAE (extracted from ARPAE environmental geospatial website: <https://arpae.it/cartografia/>).

In the Agosta field area the average calibrated vertical velocity of the points falling within a radius of about 2 km resulted  $-4 \pm 1.5$  mm/yr, while in the area of Dosso degli Angeli  $-5.5 \pm 1.5$  mm/yr. Therefore, according to these results, Eni assumed for the whole area under examination, an average subsidence component not attributable to gas extraction of  $-5$  mm/yr.

According to this value, Eni elaborated a simulation of subsidence induced by the production of Agosta and Dosso degli Angeli: at Agosta and for the worst scenario, 17 cm of anthropogenic lowering are to be expected in 2030, to which further 6.5 cm ( $5$  mm/yr  $\times$  13 years) will occur because of natural subsidence.

But this scenario is not in agreement with the subsidence data collected by ARPAE, in particular with the estimation of the current ground motion, i.e., that before the beginning of production at Agosta field. According to the ARPAE survey of subsidence for the years 2006–2011 (SqueeSAR RADARSAT Asc data), basically all the territory is free from significant land subsidence, and in the Agosta area the vertical velocity rate is estimated to be around 0 mm/yr. The Region territory was divided in 6 sub regions (sites) for processing. The SqueeSAR velocities were calibrated with the CGPS network of Emilia Romagna Region (Figure 8.1.3), consisting of 17 permanent stations, belonging to three different geodetic infrastructures. ARPAE used these stations to define the datum for the interferometric analysis. ARPAE used six of these permanent stations for the calibration of the interferometric data. Around each GPS station, SqueeSAR scatterers were selected and the average of their velocities, weighted on the basis of their coherence, was computed. Then, the differences with the GPS data (datum) were calculated. These differences were minimized by means of a calibration procedure that consisted in removing a low frequency velocity component, mainly due to orbital errors (from a geometric point of view, a plan was determined and applied). In this way, the average ground motion velocities of SqueeSAR data were referred to the absolute reference system made up of CGPS stations. Successively, the vertical component velocities of a



further ten GPS stations were used as checkpoints with respect to the calibrated velocities. Statistical procedures were also applied and at the end of the process, the average rate of lowering estimated by ARPAE for the period 2006–2011 in the area of Dosso degli Angeli is about -2 mm/yr, different from that estimated by the proponent of about -6 mm/yr in a radius of 150 m from the Smarlacca CGPS. Finally, in the Agosta area, the ARPAE map of vertical velocities for the period 2006–2011 shows values within 0 and +2.5 mm/yr (Figure 8.1.2c). Recently, ARPAE has published a new subsidence survey based on 2011–2016 InSAR data. The Agosta area shows again slightly negative velocities (between 0 and -2.5 mm/yr; Figure 8.1.4b).

In the process that led Eni to estimate the value of -5 mm/yr, a decisive role played the calibration carried out using the Smarlacca CGPS station, located about 15 km from the Agosta site and not included in the network of 17 CGPS stations used instead in the calibration process performed by ARPAE.

The Emilia Romagna Region evaluated unfavorably the project, stating that the uncertainties in the comparison of the subsidence estimates provided by Eni with those carried out by ARPAE do not allow for properly assessing the actual impacts. The divergent (albeit by a few mm/yr) ground motion estimates produced by Eni and ARPAE, although both formally correct, are not comparable, having followed different procedures and, in particular, having been calibrated with different methods.

For further information on the above, reference can be made to the paper published by Comerci and Vittori (2019), reported in the Supplementary material (Section 15).

While recognizing that the possibility of measuring ground displacements with different monitoring techniques and networks makes it possible to carry out independent assessments useful for possible cross-checks, it is clear that there is a need to have a sufficiently dense and validated nationwide reference network for the calibration of InSAR data. A dense GNSS permanent national network connected to the EUREF Permanent Network (EPN) would be ideal for this purpose. Today in Italy we can count tens of different geodetic infrastructures, with more than 930 stations, of which only 28 belong to EPN. However, 677 stations participate in the EPN Densification ([http://www.epncb.oma.be/\\_densification/about.php](http://www.epncb.oma.be/_densification/about.php)). Therefore, the overall number of already functioning and potentially networkable stations is relevant, even if their spatial distribution on the territory is not homogeneous and a number of them may not meet the basic technical requirements, especially on monumentation, as defined in specific guidelines.

The European Commission, in the framework of the Copernicus Programme, in 2018 started financing the implementation of the European Ground Motion Service (EGMS), aimed at providing reliable and timely information regarding natural and anthropogenic ground motion phenomena in Europe. The objective is to detect ground displacements (including land subsidence) with millimetric accuracy, by applying the SAR technology taking advantage of the images continuously acquired by the ESA Sentinel-1 satellites. The European Environmental Agency (EEA), which is entrusted with the realization of the service, is exploring the availability of in-situ networks exploitable for the validation and the calibration of the ground motion data. The first release of EGMS is expected in 2022 and will have an annual update (see also Crosetto et al., 2020).

Similarly, at national level, the implementation of a Ground Motion service, based on interferometric data and designed as a Mirror Copernicus Downstream Service, is one of the expected products of the ongoing Italian Space Economy Strategic Plan.

Such initiatives, at European and national level, could offer the opportunity to structure a reliable GNSS network, specifically dedicated to calibrating InSAR data, starting from



the large number of stations already existing in Italy, which would need to be combined and harmonized.

The uncertainties in the evaluation of ground deformations are not only due to the techniques of ground motion and calibration applied, but also to the complexity of the phenomenon itself characterized by the combination and overlapping of natural and anthropogenic processes, acting in different spatial and temporal intervals. Understanding these processes and quantifying their contribution to the ground deformations can significantly contribute to better assess this complex phenomenon. The Po Basin represents an interesting area where analyze such processes and their interactions; for this reason, several studies investigated subsidence causes in this area. Carminati et al. (1999 and 2003b) studied the Plio-Pleistocene sedimentary infilling of the basin to discriminate the natural short- and long-term components of subsidence, emphasizing the role of the flexure of the Adriatic Plate beneath the Tyrrhenian Plate (tectonic process), the compaction of sediments, and sediment isostasy (sediment-related processes). These authors also quantified the contribution of the isostatic rebound related to the load loss after the Alpine glaciers melting of the Last Glacial Maximum.

Teatini et al. (2011) focused their study on the natural short-term component of the subsidence, pointing out the correlation between the subsidence rate and the age of the shallower sediments of the Po River delta: Late Holocene mud sediments consolidation is indicated as the main cause of the present-day subsidence.

Similarly, Vitagliano et al. (2020) correlated subsidence values with the thickness of the last Holocene prograding sequences, pointing out the need for modeling the compaction process affecting this sequence which might help to discriminate the contribution of shallow sediment compaction and tectonics-driven mechanisms to the present-day subsidence.

However poor attention has been devoted to the tectonic component of ground deformations related to the activity of blind faults, despite they are very frequent in the Po Basin, they control the main O&G fields, and are responsible for seismic events (e.g. Emilia 2012 seismic sequence). Computing this contribution, even if local and sometimes elusive, can also help to better quantify the present-day subsidence, together with the fault activity characterization.

Maesano & D'Ambrogi (2016) proposed a workflow based on sequential 3D decompaction and restoration in the Piadena – Solarolo area (central Po Basin) (Figure 8.1.5), where the presence of an external fault-propagation fold related to the Emilia arc was already known (Pieri & Groppi, 1981; Bigi et al., 1990; Picotti et al., 2007; Wilson et al., 2009; Rossi et al., 2015) but no detailed studies existed on its Pleistocene activity.

In this structural situation, very common in the whole Po Basin, syntectonic deposits and growth strata are strategic to describe the basin evolution and tectonic control; furtherly decompaction (Sclater & Christie, 1980; Gutierrez & Wangen, 2005; Durand-Riard et al., 2011) and regional tilting (Carminati et al., 2003a; Bresciani & Perotti, 2014) must be taken into account to assess the vertical component that can be attributed to the local tectonic processes (Maesano et al., 2013).

The workflow, applied to a highly detailed 3D geological model (Figure 8.1.6), built in the framework of the EU-funded GeoMol Project (GeoMol Team, 2015) and furtherly updated during the GeoEra HotLime Project, which includes six stratigraphic horizons in the last 1.5 Myr and 3D blind thrust surfaces (Solarolo Fault System in the HIKE Fault



Database - <https://data.geoscience.earth/ncl/geoera/hotLime/faults/4371>, allows calculating the local long-term syntectonic vertical signal in a general subsiding basin.

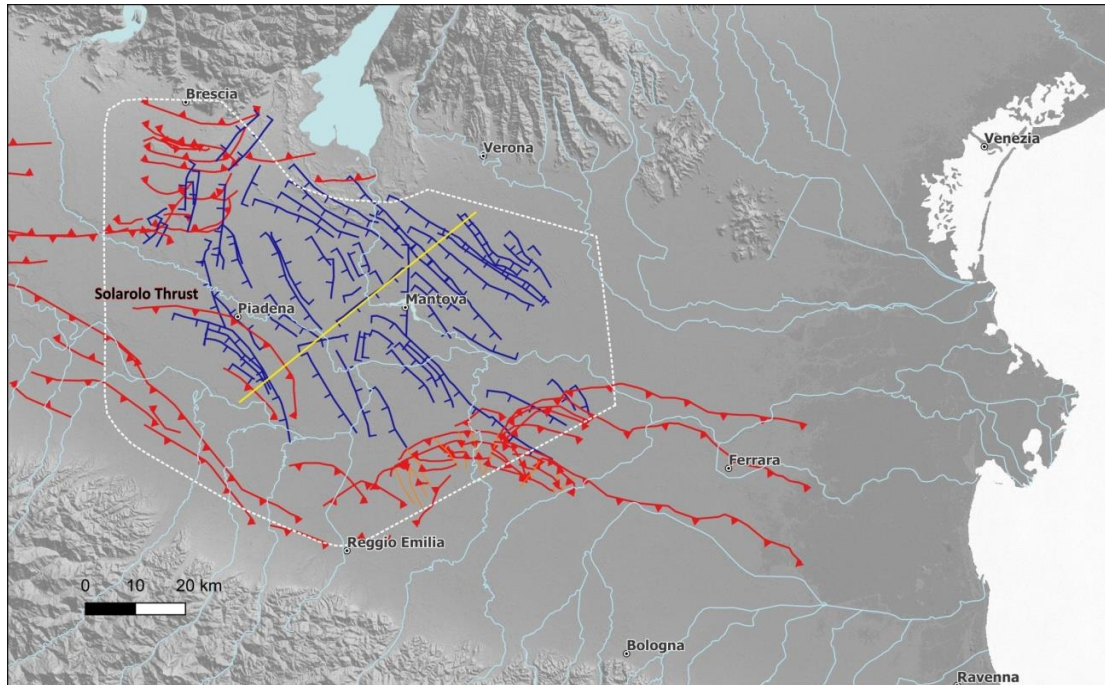


Figure 8.1.5: Central-eastern portion of the Po Basin; the dashed white line bounds the area where the sequential 3D decompaction and restoration workflow was applied, the yellow line represents the position of the slice shown in Figure 8.1.6. The faults are mapped with their upper tip derived from 3D geological model (GeoMol and HotLime Projects). Blue line: normal fault, red line: thrust, orange line: minor fault.

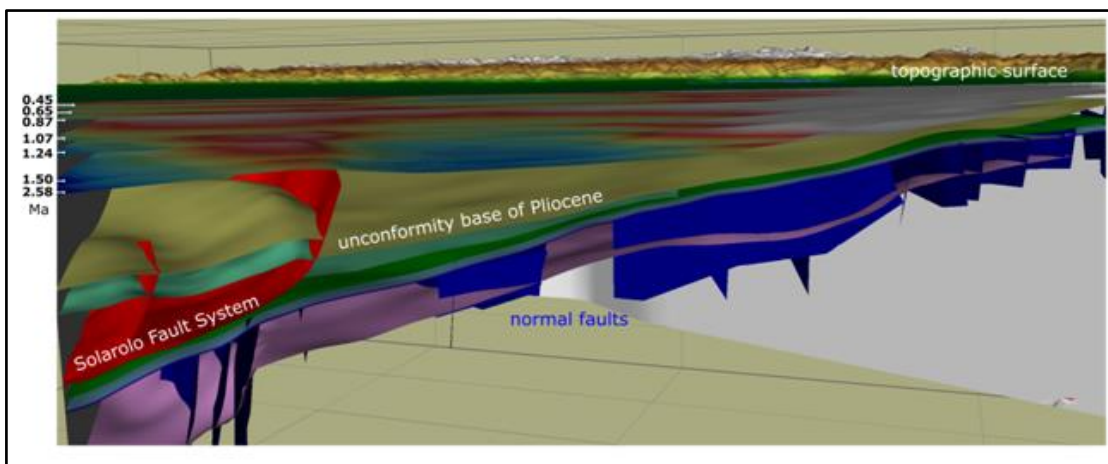


Figure 8.1.6: N230 slice of the 3D geological model of the Piadena - Solarolo area (see Figure 8.1.5 for the position), after GeoMol Project (GeoMol Team, 2015); vertical exaggeration 1.5x. All the faults of this 3D model are also included in the European Fault Database (HIKE Project). The workflow (Figure 8.1.7) consists of successive steps of restoration of the modeled stratigraphic surfaces: i) unfolding, ii) decompaction and unload, and iii) removal of regional tilting and measure of the residual vertical separation along with antiformal



structures, controlled by blind fault. The vertical separation is calculated from the anticline crest and the adjacent syncline bottom.

As stated by Maesano & D'Ambrogi (2016), the decompaction of sediments (volume between two stratigraphic horizons) is necessary to remove the effects of rock volume change due to porosity reduction in response to the load of younger sedimentation. Sediment compaction can locally represent the main cause of natural subsidence (Teatini et al., 2011), but there are documented cases of differential compaction driven also by human activity (Stramondo et al., 2007; Baldi et al., 2009, for the Po Plain).

In areas affected by fault-propagation folds related to blind thrusts, the decompaction effects are larger in the depocenters (syncline axes) where the sedimentary load is greater than in the structural culminations (anticline crest axes); not considering the effects of decompaction leads to an overestimation of the vertical movements (calculated, for the Ferrara Arc, in more than 50% by Scrocca et al., 2007) because the effects of decompaction are more evident in syntectonic layers that were subjected to differential vertical load. From a short-term perspective, this can affect the calculation of subsidence in areas characterized by active faults.

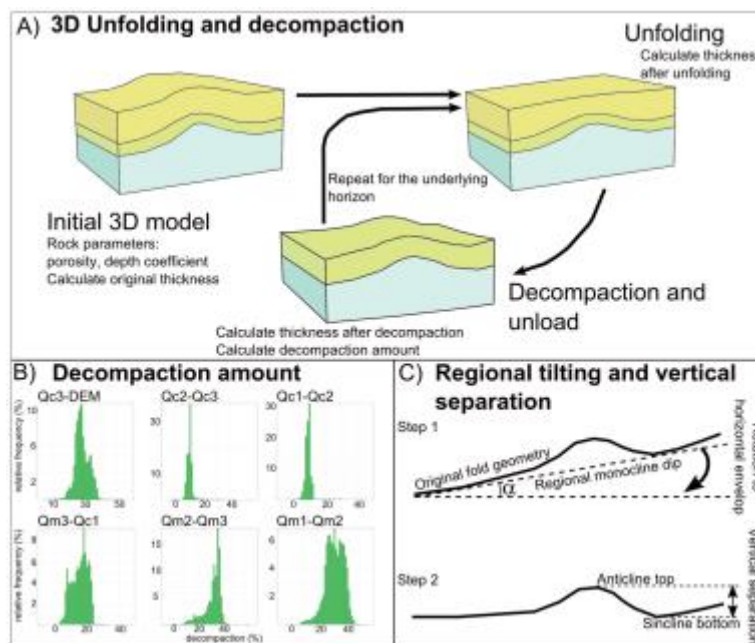


Figure 8.1.7: Workflow proposed by Maesano & D'Ambrogi (2016): from the original 3D model, successive steps of unfolding and decompaction are performed; B) decompaction amount for the six Pleistocene units adopted in the study; C) scheme of the recovery of the regional tilting (dip monocline) for the calculation of the vertical separation from the anticline top and the adjacent syncline bottom.

According to the availability of a well-constrained 3D geological model, the proposed workflow allows detection also of very little vertical ground movements related to long-term blind fault activity, although the region is affected by overall subsidence (Table 8.1.3).

	Myr	Sedimentation rate	Uplift rate
--	-----	--------------------	-------------



Qc3-DEM	0.45-today	$0.40 \pm 0.05$	0.12	$0.06 \pm 0.05$
Qc2-Qc3	0.63-0.45	$1.04 \pm 0.17$		$0.24 \pm 0.12$
Qc1-Qc2	0.87-0.63	$0.54 \pm 0.11$		$0.15 \pm 0.09$
Qm3-Qm2	1.07-0.87	$2.91 \pm 0.25$		$0.26 \pm 0.11$
Qm2-Qm3	1.24-1.07	$2.71 \pm 0.28$		$0.58 \pm 0.15$
Qm1-Qm2	1.50-1.24	$3.59 \pm 0.21$		$1.20 \pm 0.12$

Table 8.1.3: Sedimentation and tectonic uplift rate (mm/yr) calculated for six Pleistocene intervals (Maesano & D'Ambrogi, 2016).

To contribute to the better estimation of the natural component of the subsidence this approach needs i) a well-constrained 3D geological model with high detail geometry of the Pleistocene-Holocene sedimentary boundaries to obtain the thickness of the units (Figure 8.1.8), ii) high detail 3D geometry of the thrusts, as modeled in the HotLime and HIKE projects (Figure 8.1.9), ii) the sand/shale percentage for each unit, iv) well-defined chronological constraints unit ages.

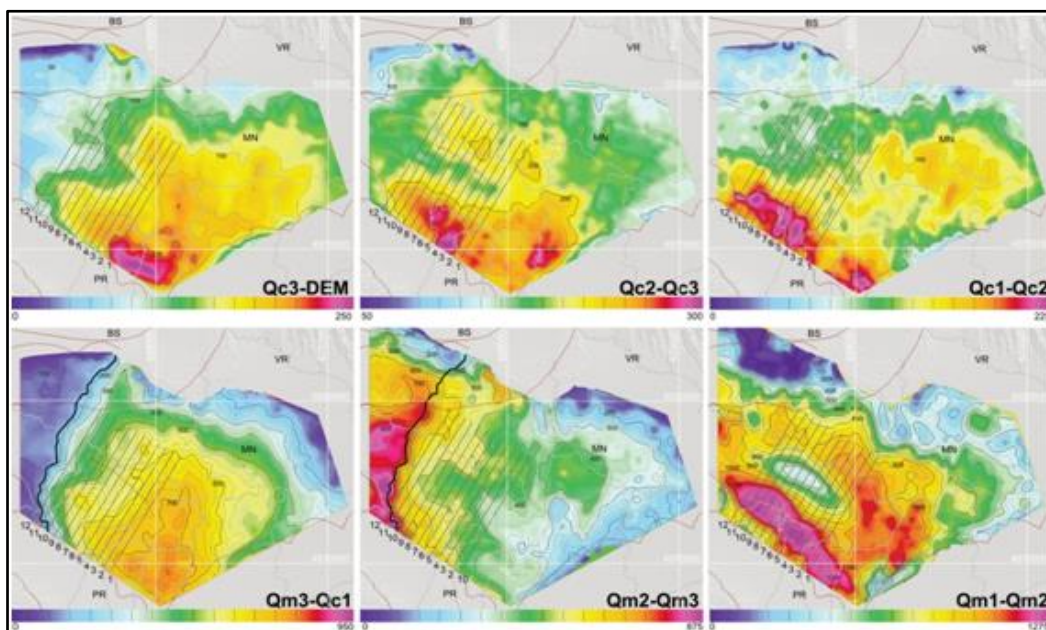


Figure 8.1.8: Thickness maps of the units confined by the Pleistocene unconformities (see Figure 8.1.5 for the position and Table 8.1.3 for the age). Isopachs are displayed each 25 meters except for the Qm1-Qm2 map where contours are 50 meters spaced (Maesano & D'Ambrogi, 2016).

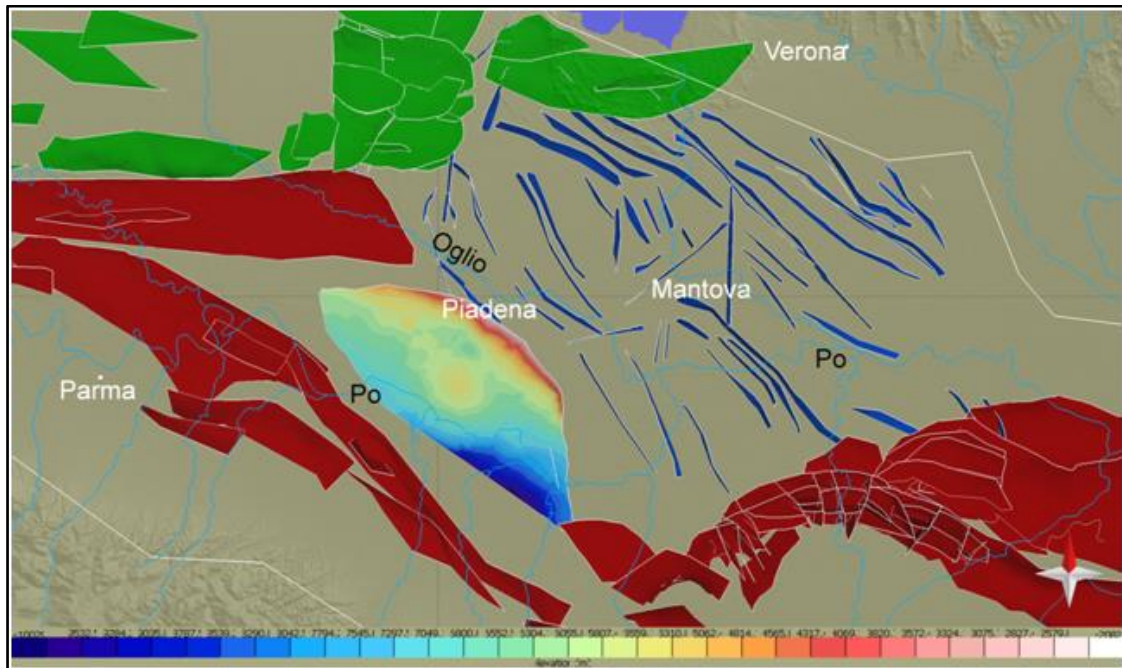


Figure 8.1.9: Map view of the 3D modeled faults of the central Po Plain, after GeoMol and HotLime projects (white line: boundary of the modeled area). Green surface: Southalpine thrust, red surface: Northern Apennines thrust, blue surface: normal fault. The Solarolo thrust (Northern Apennines) is colored according to depth.

The uncertainties associated with this method influence the calculation of the rates; in generally subsiding basins (e.g. the Po Basin) affected by tectonic-related uplift rate systematically one order of magnitude lower than the long-term sedimentation rates, the evaluation of uncertainties is particularly important.

As reported in Maesano & D'Ambrogi (2016), sedimentation and uplift rates are not independent observations but rather derived quantities; they are affected both by epistemic uncertainties and by the propagation of the errors affecting the raw data, some of which are not always measurable. The calculation of the uncertainties for each sedimentation and uplift rate value is obtained as the sum of the relative individual uncertainties on the age and the thickness or vertical separation. The uncertainty in the age can be considered as the precision in the calibration of the corresponding MIS stage; since for these studies the second decimal precision is necessary, Maesano & D'Ambrogi (2016) adopted a conservative range of uncertainty of  $\pm 0.01$  Myr. For the measurement of thickness and vertical separation, the resolution of the seismic profiles ( $\sim \pm 20$  m, after depth conversion) is adopted as the interval of confidence in the measurement.

Following this approach, vertical separation related to slow deforming faults can result at the limit of the resolution of the proposed method; nevertheless, this methodological approach can be applied in a wide range of sedimentary basins to have a quantitative evaluation of both sedimentary and tectonic processes, and to discriminate them from the anthropic signal.

Unfortunately, for the area where a subsidence map is available (Emilia-Romagna Region) the existing 3D geological model includes, at this stage, only the main thrusts



and two modeled horizons in the Pliocene-Holocene interval, on the other hand, a 3D geological model with the needed level of details of the Pleistocene units is still lacking.

## 8.2 Po Plain 2

### METHODOLOGY AND ANALYSIS

In this project, PS-InSAR of ERS SAR-1/2 data has been statistically analysed to generate Iso-Kinematic Map (IKM, Morelli et al., 2008, 2011), and their Iso-Kinematic boundaries, to compare the tectonic activity of faults vs. the crustal mobility at the land surface. The IKM represented land sectors, whose areas span from tens to hundreds square kilometres, expressed in high and low values of  $Z(Gi^*)$  (see below) and characterized by homogeneous kinematic behaviour. These land sectors display relative movements toward and away from satellites and are delimited by the different types of boundaries (IKB). The geometry of IKB can be very straight or curvilinear, very narrow (less than one kilometre) with high velocity gradient across them or very large (tens of kilometres) with gentle velocity gradient (Figures 8.2.1, 8.2.2, 8.2.3, 8.2.4). Different geological meanings can be inferred for the IKB, depending on the geometry and velocity gradient observed across them.

The boxplot diagrams used to describe the statistical distribution of PS data set of ERS SAR-1/2 (Figure 8.2.2) are characterized by a large amount of negative and positive outliers. In particular, the PS boxplot diagrams of the geological sector 1 (Figure 8.2.3) show a symmetric distribution of the data; conversely, the boxplot diagrams of the geological sector 2 show a negative and positive skewed with an asymmetric distribution for two different scenes (satellite track/frame: 480/2709 and 480/2691) Moreover, all data are characterized by high values of negative and positive outlier reaching respectively up to  $-20$  mm/year and up to  $+17$  mm/year.

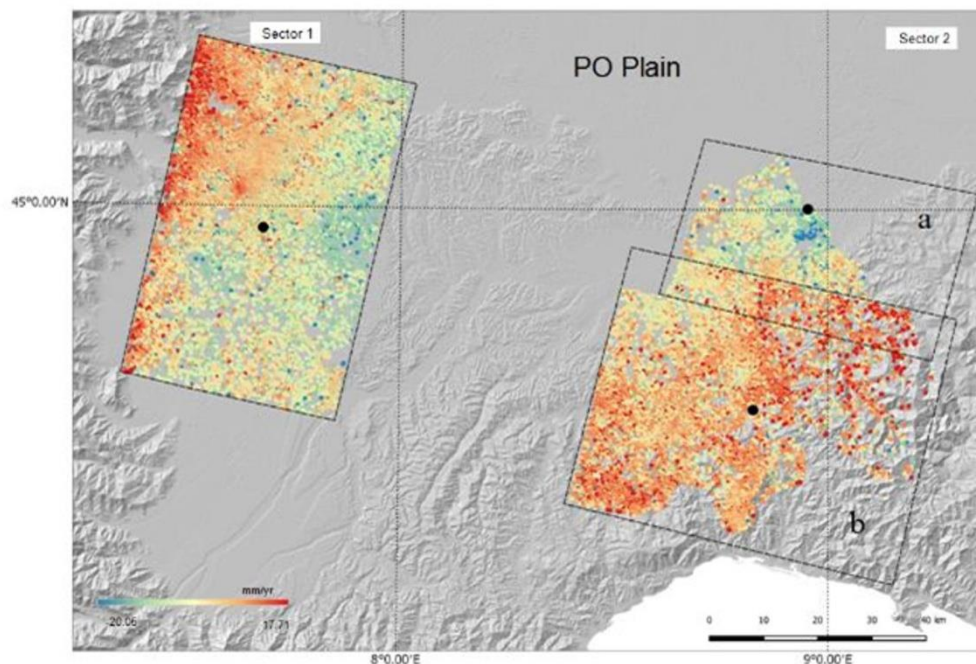


Figure 8.2.1. velocity-PS distribution in sectors 1 and 2. The black dashed indicate the fixed reference points; a and b areas represent two different satellite scenes.

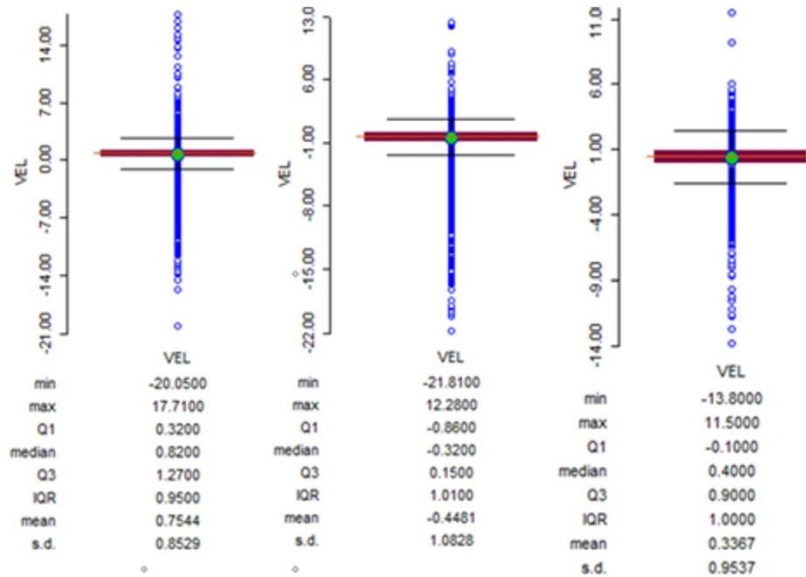


Figure 8.2.2. Boxplot of the PS data in the studied geological sectors. a. sector 1; b and c sector 2.

Although the high negative velocity values are probably due to the occurrence of landslides i.s., the positive values seem to be too high with respect to the known average velocity of the tectonic crustal mobility in the orogenic belts. We remark that this work does not focus on analysis of absolute PS-velocity values, but only on comparing PS velocities of different iso-kinematic areas. The interpretation of the absolute PS-velocity values is still uncertain, mainly because the PS values are relative to a fixed reference point (see Figure 8.2.1), and the red and blue colours shown in the following figures simply represent areas with relative movement toward and away from satellite.

A first interpolation between PS was done by an ordinary kriging interpolation that relies on the spatial correlation of the data, as inferred by variography analysis, to determine the weighting values. This is a more rigorous approach to modelling, as the correlation between PS-velocity points gives the estimated velocity value at an unsampled point. Semivariogram values for different lags were derived from the semivariogram model fitted with the measured PS values. Geostatistical maps show a significant variability at local scale with larger areas (from 2 to 10 km<sup>2</sup>) characterized by strong negative velocity (ranging between -21 and -13 mm/year) and smaller areas (from 1 to 2 km<sup>2</sup>) with strong positive velocity (ranging between to +11 and +17mm/year). Field analyses performed on these areas allowed suggesting that the strong negative values correspond to deep seated gravitational slope deformation and landslides and small areas where human activities (i.e., heavy industrial buildings or local water pumping) induce subsidence. Since these anomalies may mask the crustal tectonic mobility, a further spatial statistical analysis (Getis & Ord, 1992) was performed. This technique has the advantage to detect “pockets” of PS velocity spatial association at different scales. The statistic is calculated as follows:



1:

$$G_i^*(d) = \frac{\sum_j w_{ij}(d)x_j}{\sum_j x_j}$$

where  $w_{ij}(d)$  is a binary spatial weight matrix with ones for all links defined as being within distance  $d$  of focal point  $i$ ; all other links are zero. The numerator is the sum of all  $x_j$  within  $d$ ; the denominator is the sum of all  $x_j$  in the whole spatial domain.  $G_i^*(d)$  is a measure of concentration or lack of concentration of the sum of values associated with variable  $X$  in a given region.

By taking the statistic minus its expectation, divided by the square root of its variance, a new measure is obtained (Ord & Getis, 1995):

2:

$$Z(G_i^*) = \frac{G_i^*(d) - E(G_i^*(d))}{\sqrt{\text{Var}(G_i^*(d))}}$$

$Z(G_i^*)$  indicates how many standard deviations  $G_i^*(d)$  differs from its expected value  $E(G_i^*(d))$ , introducing a measure of significance in the former statistic (equation (1)). The higher the absolute value of  $Z(G_i^*)$  is, the more confident we are that the  $G_i^*(d)$  value is anomalous, and so the sum of the  $x_j$  values within distance  $d$ . Concentration of positive (hot spot) and negative (cold spot) significant values of  $Z(G_i^*)$ , identify clusters of anomalous PS-velocity values. Once the statistic is computed, the choice of  $(d)$  values must be done. When using a distance-based neighbourhood, the distance  $(d)$  specified is based on knowledge of the features and investigated phenomenon. With a larger distance, it is possible to have few large clusters, while a smaller distance gives several smaller clusters. It must be accepted that there is no correct neighbour distance: in fact, different  $d$  values allow exploring the phenomenon at multiple spatial scales. To define the range of  $d$  value, three elements were taken into consideration:

- the scale as inferred from the geological model and geomorphological features (for example the medium length and relative distance of the main regional faults, the density of the segments of rivers drainage, the drainage patterns, the gradient and profile of slopes, and the length and distribution of remotely sensed lineaments);
- the maximum extent of spatial autocorrelation as showed by variography analysis;
- the extent of the area under investigation in order to prevent border effects.

$Z(G_i^*)$  was calculated for three different distances  $d$ : 10 km, 5 km, and 2.5 km. For this study the  $d=5$  km resulted as the proper distance values to generate the IKM for both sectors. This analysis allowed generating IKM to be compared with the present knowledge of tectonic mobility of the study region. Attention has been focused on the boundaries of the iso-kinematic areas (IKB), namely to their geometry and the velocity gradient across them (Figures 8.2.3 and 8.2.4).

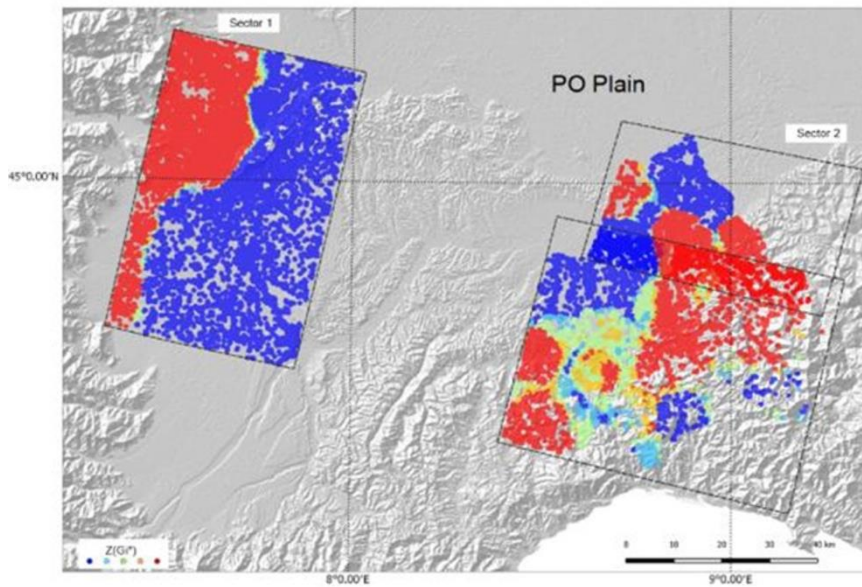


Figure 8.2.3. Hot Spot results calculated with  $d=5$  km: red and blue points represent respectively high and low  $Z(Gi^*)$  values in relation to the expected value obtained from equation 2 (see text).

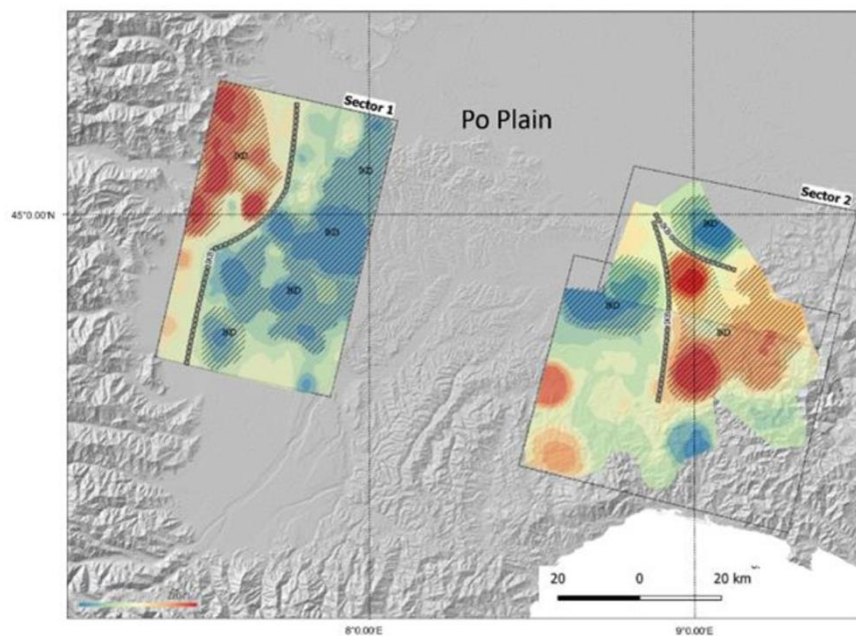


Figure 8.2.4. Iso-kinematic map, expressed in high and low values of  $Z(Gi^*)$ , respectively in red and blue colour areas. Dashed black lines are the IKBs, dashed areas are the Iso-Kinematic Domains IKDs.



## **COMPARISON WITH THE GEOLOGICAL DATA AND SEISMIC LINE INTERPRETATION**

Iso-Kinematic Domains (IKD) and Iso-Kinematic Boundaries (IKB) have been compared to geological data. Nevertheless, the Iso-Kinematic domains represent land sectors characterized by homogeneous kinematic behaviour and the Iso-Kinematic Boundaries are statistical limits that bound them. The interpretation of IKB and IKD are based on an integrated analysis of surface and subsurface with geological/geophysical data.

As reported in task 2.3 and task 3.2 of this project, the objective is to evaluate the possibility of identifying hidden faults or faults with a small throw, in depth that induce deformations of the ground by InSAR interferometric data analysis.

### *Geological data and seismic line interpretation*

Stratigraphic and tectonic analysis has been carried out through the integration of geological surface data (GeoPiemonte map - Piana et al. 2017a; 2017b) and subsurface data with the interpretation of three reflection seismic lines (Figures 8.2.5, 8.2.7, 8.2.8 and 8.2.9). This latter has been provided by ENI SpA under a confidentiality agreement (HotLime GeoEra project) and interpreted in 2018-2019.

Three reflection seismic lines have been analysed to ca. 2s TWT. The stratigraphic logs of exploration wells (published by AGIP, 1972; AGIP, 1994), have provided a general calibration for seismic interpretation even if, due to the lack of information on interval-velocities, time-depth conversion has been achieved by using average values of 1600-1800 m/s for Quaternary successions, 1800-2000 m/s for Pliocene successions and 2500-3500 m/s for Messinian successions.

Correlation between subsurface seismic lines and surface geology has been based on comparison with the geological map of Piemonte (Piana et al., 2017a; 2017b) and relative faults database (Figure 8.2.5).

Seismic profiles have been analysed based on conventional seismic-stratigraphic criteria (Mitchum et alii, 1977; Badley, 1987). The analysis of reflection terminations has allowed the identification of the major tectonic structure and of the unconformities of regional extent. The seismic-scale unconformities have been correlated to the nine major discontinuity surfaces (D1 to D9 see Figures 8.2.6 and 8.2.7) that are recognizable in the outcropping domains and mapped in the GeoPiemonte map, allowing a feasible identification of the 9 main synthems (see Figures 8.2.6, 8.2.7 and 8.2.8).

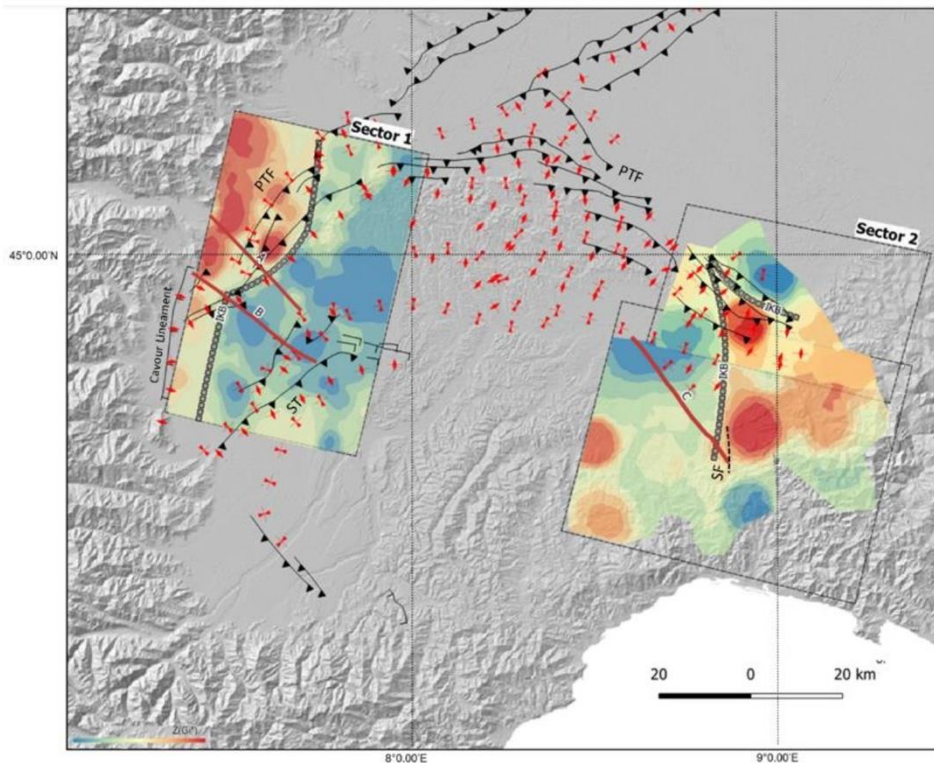


Figure 8.2.5. Iso-kinematic map and Iso-Kinematic Boundaries (IKBs) of the sector 1 and sector 2 with tectonic framework of the main faults and thrust-fold-belt (black lines indicate the blind thrust and in red lines indicate asymmetric anticline-syncline folds pair) of Western Po Plain masked at surface by Quaternary deposits. Padane Thrust Front (PTF); Scrvia Fault (SF), Savigliano Thrust (ST). A, B, C traces of the seismic cross section in Figure 8.2.6.

### *Sector 1*

Seismic cross sections (Figures 8.2.6 and 8.2.7) reveal the deformation style of the subsurface Cenozoic succession throughout the western part of the Western Po Basin, the Torino Hill domain and the Moretta sub-basin. In these contiguous geological domains, the sedimentary units of the syn-orogenic basins (both the Eocene-Miocene succession of the TPB and the Pliocene-Pleistocene one) are deformed by regional scale NE-SW trending gentle to open fault-propagation folds, with sub-vertical to highly inclined, SE dipping, axial surfaces and axes gently plunging towards SW.

In the study area these correspond to the Torino Hill anticline, in the centre, and the Western Po Basin and Moretta synclines to the NW and SE, respectively.

In particular, the Torino Hill is an open faulted anticline, whose exhumed portion is situated in the homonymous reliefs, to the east of the Torino urban area (Bonsignore et al. 1969; Festa et al., 2009). This structure is related to the propagation of the PTF NNW-vergent thrust system, which drives the local superposition of Oligocene-Miocene succession onto the Pliocene sediments.

Seismic cross section allows to recognize two major structural trends corresponding to the N-verging Padane Thrust Front systems (red line Figures 8.2.6 and 8.2.7). In details the figure shows a major NW vergent thrust and a minor one structure resulting in a very



steep geometry developed behind the axial plane of the TH antiform. In particular, the available seismic line shown that these thrust systems are active until Pliocene and Pleistocene times, as it is shown by the crosscutting of D7 (base Zanclean) and D8 (intra-Zanclean) unconformities and bending of D9 (Gelasian) one (igs.s 7 and 8). Nevertheless, Michetti et al. 2012 showed by re-interpreting the geological cross section across the TH, that the PTF cuts through the whole sedimentary sequence, probably also displacing the Holocene sediments. Moreover, geomorphological evidence of recent tectonic activity can be found on the northern slope of TH, where there are uplifted middle-to-late Pleistocene fluvial terraces and relics of meandering river courses (Vezzoli et al. 2010). On this basis, Barbero et al. (2007) estimated an uplift rate of 0.8 mm/yr to 1.0 mm/yr. This is consistent with the geodetic levelling that was undertaken in the period of 1897 to 1957, which identified a contemporary uplift rate of ca. 3 mm/yr for the whole TH sector (Arca and Beretta 1985). Beneath the Torino metropolitan area, thrust faults of the PTF system reach the surface, and the bedrock in the hangingwall is generally only a few meters below the topographic surface (Michetti et al. 2012). Above the bedrock, there is only a thin cover of Latest Pleistocene to Holocene fluvial sediments (Carraro 1976, Forno 1982, Dela Pierre et al. 2003). In this case, the depositional and/or erosional processes have not kept pace with the tectonic uplift: in the inner sector of the range, the older features are progressively more uplifted, while in the adjacent sector of the plain, there are only incipient reliefs or terraces (e.g., the small isolated hill of Trino, see Michetti et al. 2012, a relief to the east of the analysed sector).

Along the internal border of the Alpine arc, the seismic lines (pink lines in Figures 8.2.6 and 8.2.8) suggest the presence of a very steep N-S striking fault system. This structure, which corresponds to the south with the so-called "Cavour's structure" (sensu Ghielmi et al. 2019) represents a high angle transpressive feature with WNW vergence and a maximum vertical displacement of about 200-300m (Ghielmi et al. 2019). The fault tip seems to cut the whole sedimentary sequence, probably also reaching and displacing the Holocene alluvial sediments. Furthermore, this structure seems to reactivate the southern part of the Col del Lis-Trana Deformation Zone.

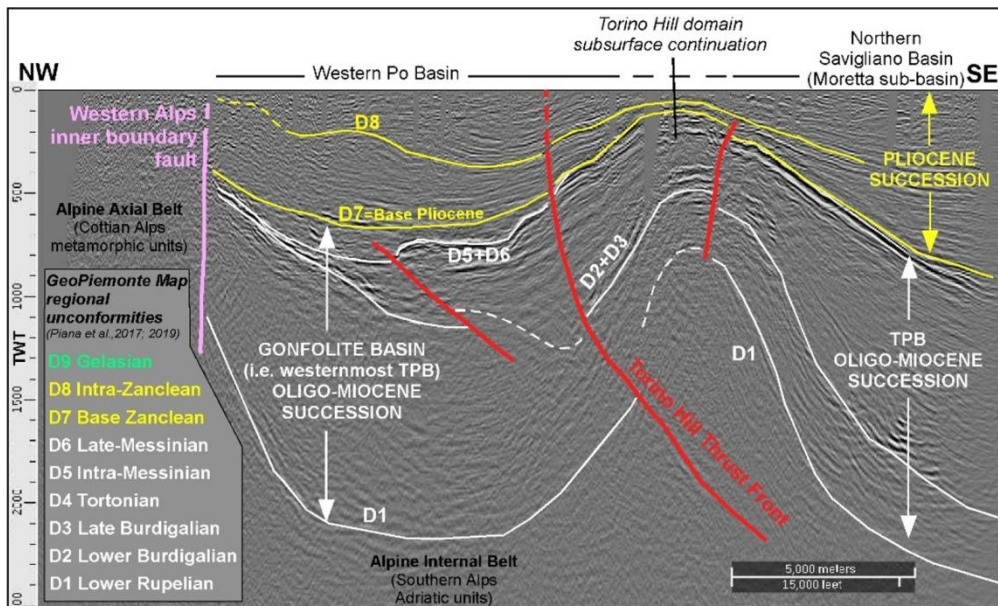


Figure 8.2.6. Line drawing of seismic line A in sector 1. Traces of the seismic lines are in Figure 8.2.5, the unconformity codes have been recognized between easternmost part of the Cottian Alps and the subsurface western termination of the TH domain and on the back of the TH domain and correspond to those proposed in the Geo Piemonte Map (Piana et al., 2017a; 2017b) Traces of the N-verging Padane Thrust Front systems and tectonic lineaments consistent with interpretation of the “Cavour structure” on surface.

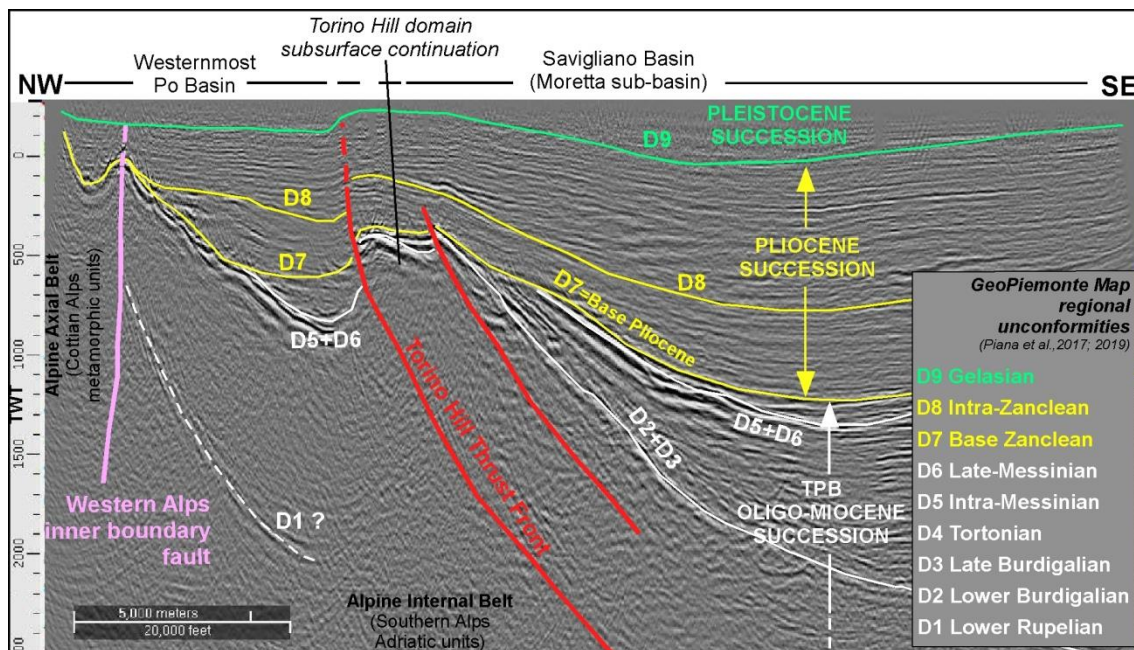


Figure 8.2.7. Line drawing of seismic line B in sector 1. Traces of the seismic lines are in Figure 8.2.5, the unconformity codes have been recognized between easternmost part of the Cottian Alps and the subsurface western termination of the TH domain and on the back of the TH domain and correspond to those proposed in the Geo Piemonte Map (Piana et al., 2017a; 2017b). Traces



of the N-verging Padane Thrust Front systems and tectonic lineaments consistent with interpretation of the “Cavour structure” on surface.

### Sector 2

The seismic cross section (Figure 8.2.8) reveals the 7 unconformity bounded stratigraphic units better documenting the gently northwest-dipping monocline in the southern margin of the Alessandria Basin. Starting from the D4 Tortonian unconformity, the succession displays an important SE-ward thickness decrease and syn-sedimentary angular unconformities related to the uplift of the basement to the SE.

Along the internal border of the Apennines tectonic belt, seismic cross section (Figure 8.2.8 green and red lines) reveal the traces of the buried N-S trending vertical faults system, which are not well known at present. These traces could correspond to the surface to Scrivia and Lemme tectonic lineaments, although the poor quality of the shallower part of the seismic line does not allow to clearly constrain this hypothesis. The existence of a tectonic lineament corresponding to the Scrivia River valley, as well as the analysis of fluvial dynamics and alluvial sediments distribution in order to assess Pleistocene-Holocene differential tectonic uplift and neotectonic activity along it, was already outlined by several authors (see par. 2.1).

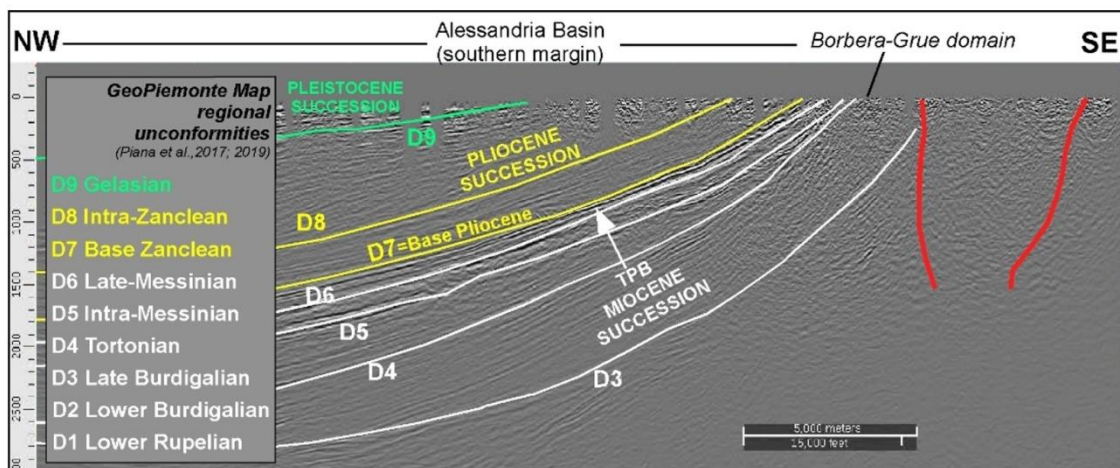


Figure 8.2.8. Line drawing of seismic line C in sector 2. Traces of the seismic lines are in Figure 8.2.5, the unconformity codes have been recognized in the Alessandria Basins and correspond to those proposed in the Geo Piemonte Map (Piana et al., 2017a; 2017b). Traces of the tectonic lineaments consistent with interpretation of the faults Scrivia and Lemme trends on surface.

### **COMPARISON WITH SEISMOLOGICAL DATA: SEISMICITY AND FOCAL MECHANISMS**

Relations between seismic activity and faults were investigated by selecting the best located earthquakes from the database of the instrumental seismicity recorded by the Seismic Network of the Western Italy (RSNI) for the period 1982-2012 and on the historical data reported by Boschi et al. (2000). The magnitude spans from  $M_L$  1.4. to 4.9 (table 1). The distribution of the hypocentres, with maximum horizontal and vertical location errors of 3 km and available focal mechanisms, were compared with the fault



pattern in sector 1 and sector 2 in map view (Figure 8.2.9 and table 1). For the aim of this study the depth of the hypocentres analysed is limited to the upper 10 km.

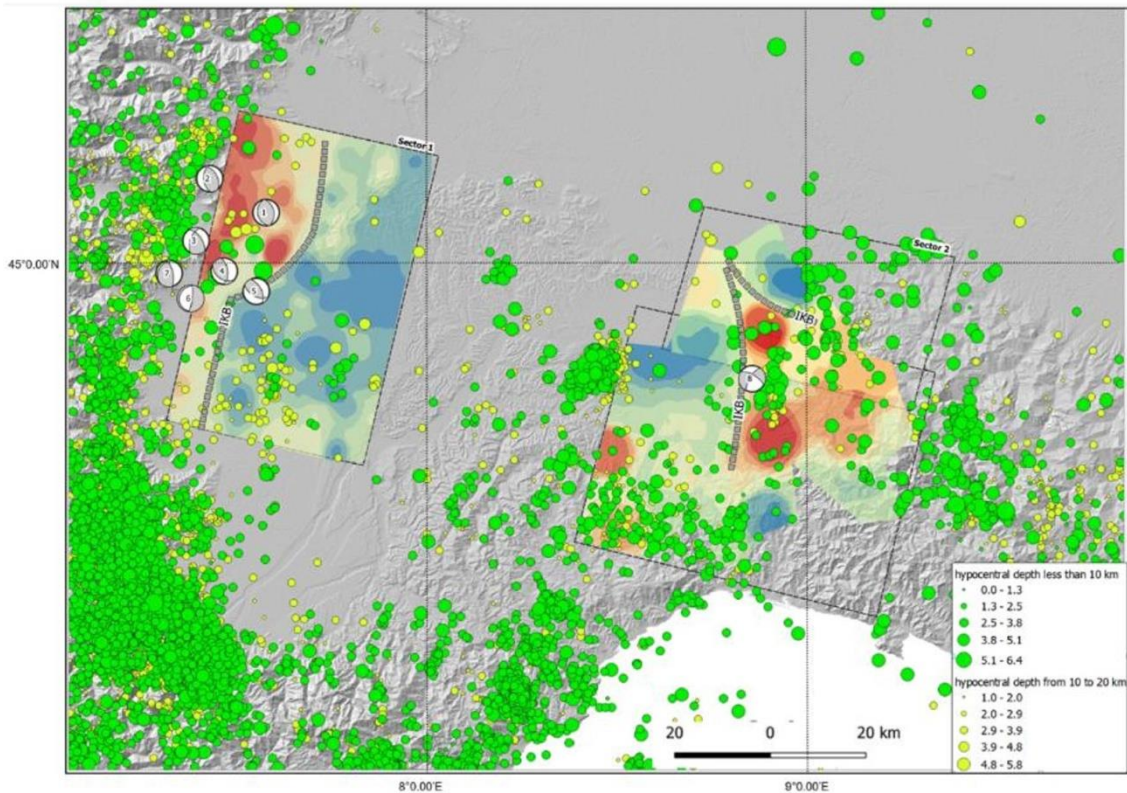


Figure 8.2.9. Map of instrumental and historical seismicity that includes the westernmost Po Valley, the internal border of the western Italian Alps (Cozie) and the northern Apennines and the Ligurian Alps from the database of the seismic network of the North-Western Italy (RSNI). Green circles represent shallow seismicity (hypocentral depth less than 10 km) and deeper seismicity (hypocentral depth between 20 and 10 km) light green circles respectively. Focal mechanisms. Numbering corresponds to that of table 1. Iso-kinematic map and Iso-Kinematic Boundaries (IKBs) of sector 1 and sector 2.

N.	Yr	Mo	Dy	Hr	Mn	Sec	Long	Lat	Depth	ML	Az1	Dip1	Rake1	Az2	Dip2	Rake2	AzP	DipP	AzT	DipT	Ref.
1	1992	9	13	5	0	37.4	7.610	45.105	4.26	3.4	350	50	90	170	40	90	80	5	260	85	S
2	1981	2	8	4	30	10.5	7.439	45.152	5.00	4.4	335	40	60	192	56	113	266	9	153	69	E
3	1980	1	5	14	31	19.9	7.419	45.034	4.00	4.8	215	55	140	331	58	42	92	2	185	51	E
4	1990	2	11	7	7	47.8	7.476	44.987	24.00	2.7	0	65	120	126	38	43	69	15	313	59	E
5	1990	2	11	7	0	37.8	7.547	44.965	16.00	4.2	120	55	60	345	45	126	231	6	333	65	E
6	1969	10	9	3	31	36	7.400	44.950	33.00	4.2	174	11	-118	22	80	-85	299	54	108	35	P
7	1983	9	6	22	43	18.4	7.390	44.970	5.00	3.8	0	72	75	221	23	129	102	26	248	60	N
8	2003	11	04	09	26	57	8.87	44.76	8	4.7	300	71	-172	207	83	-19	162	18	255	8	U

Table 1. Locations and parameters of the focal mechanisms in Fig. 2. Yr.: year; Mo: month; Dy: day; Hr: hours; Mn: minutes; sec: seconds; Long.: longitude; Lat.: latitude; ML: local magnitude; Az1(2), Dip1(2), Rake1(2): azimuth, dip, rake of fault plane 1 (2), in degrees; AzP(T), DipP(T): azimuth and dip of P(T) axes, in degrees. Ref.: E: Eva et al., 1997; N: Nicolas et al., 1990; S: Sue et al., 1999; P: Perrone et al. 2011 U: unpublished data.



### *Sector 1*

The Figure 8.2.9 shows the distribution of a well-located hypocentral among the inner of the Cottian Alps and the western Po Plain. Except for some deeper earthquakes more diffuse in the south-westernmost Po Plain (Savigliano-Saluzzo Basin) that reach 15-25 km of depth, most of seismicity is localized at relatively shallow crustal levels (in the first 10 km). Moreover, the Figure 8.2.9 shows how most of the present seismicity is aligned along a NNE-SSW direction. This alignment of the seismicity in the literature is known as Piemonte's seismic arc (Rothé, 1941; Eva et al., 1990). In this sector 1, the aligned seismicity along the NNE-SSW direction seems to join the northern segment of the LTZ (Figure 6.2.1) while, to the south, the hypocentral are aligned along the Cavour tectonic structure and to the east, along with the PTF north-verging thrust systems. (Figure 8.2.10).

Seven focal mechanisms have been selected (from Perrone et al. 2010) where hypocentral join the traces of the mapped tectonic structures in order to constrain the geometry and kinematics of the activated faults and the present-day stress regime.

By merging sub-surface geology and seismological data (Figure 8.2.10) a good relationship between the tectonic structures, the present-day stress regime and the distribution of the hypocentral can be observed. The focal mechanisms indicate a contrasting stress regime among the inner border of the Cottian Alps and the western Po Plain. Transpressive solutions of focal mechanisms, with sub-horizontal roughly E-W trending P axes, are in fact prevalent beneath the westernmost Po Plain. Conversely, transtensive and extensional solutions, with steep P axes and sub-horizontal ENE-WSW trending T axes, are widespread along the eastern boundary of the Alpine chain.

### *Sector 2*

This sector is mainly affected by low magnitude instrumental seismicity, even if some moderate magnitude events (August 2000 and July 2001 seismic sequences, whose main shocks reached  $ML=4.8$  and  $ML=5.1$  respectively; Massa et al., 2006) have struck the Asti-Alessandria area. Other main historical earthquakes with  $ML > 4.5$  are reported on the Catalogo Parametrico dei Terremoti Italiani (GdL CPTI, 2004) in the years 1541, 1680, 1828 e 1913 (Figures 8.2.9 and 8.2.10).

A progressive decrease in the depth of seismic events is observed from west, where seismicity is mainly confined at 25-10 km depth, to east, where hypocentres are mainly concentrated in the first 10 km depth (Figures 8.2.9 and 8.2.10).

Except for earthquakes concentrated in a cluster zones at the south of the Alessandria Basin depocenter zone (outside of the map of sector 2 Figures 8.2.9 and 8.2.10), a singular trend in the distribution of hypocentral is observed. In fact, in the central part of the analysed area, the seismic events seem to be aligned along a N-S direction from the north-western Apennines to the eastern boundary of the Alessandria Basin. This alignment is sub-parallel with some valleys (e.g. Scrivia river valley), in agreement with the direction of the Scrivia Fault SF (Figure 8.2.10). Strong historical earthquakes show similar distribution of instrumental seismicity parameters (5-7 MCS, Boschi et al., 2000) (Figures 8.2.9 and 8.2.10).

The only focal mechanism available from this sector derives from the main earthquake events that occurred in the 04/11/2003, whose main shocks reached  $MW= 4.9$ . This latter shows transcurrent solutions (Figures 8.2.9 and 8.2.10) consistent with a strike-slip mechanism with two NW-SE and NNE-SSW striking nodal planes. P axis is sub-horizontal with NNW-SSE direction, while T axis is sub-horizontal and NE-SW striking (ref. <http://terremoti.ingv.it/event1428089>). A NW-SE trend of the shallow distribution of



hypocentral on the footwall of the complex PTF thrust fold systems is also well evident (Figure 8.2.10).

## UNCERTAINTY EVALUATION/ DISCUSSION

### COMPARISON BETWEEN GEOLOGICAL/GEOPHYSICAL AND SEISMOLOGICAL DATA WITH ISO-KINEMATIC DOMAINS AND ISO-KINEMATIC BOUNDARIES

Iso-Kinematic domains and their boundaries have been compared with the available geological, tectonic and seismological data.

Iso-Kinematic domains represent land sectors characterized by homogeneous kinematic behaviour and the Iso-Kinematic Boundaries are statistical limits that bound them. Boundary geometry can be very straight or curvilinear, very narrow (less than one kilometre) with high velocity gradients or very wide with gentle gradients. Different geological meanings can be inferred for the Iso-Kinematic Boundaries, depending on the geometry and velocity gradients observed across them.

#### *Sector 1*

The IKM (Figure 8.2.10) show a differential uplift and crustal mobility between the inner Cottian Alps and the Western Po Plain that included three major tectonic structures: the NS tectonic structures dissecting the inner sector of the Alpine chain, such as the LTZ sub-vertical composite structure and the Cavour tectonic lineament and western termination of the N-verging PTF complex thrust fold systems (Figure 8.2.10). In particular, in the southern part of the sector 1, the Iso-Kinematic Boundary runs close to the trace of the Cavour tectonic lineament and the LTZ faults systems while in the northern part, where the PTF are masked at surface by the fluvial deposits of the western Po Plain, this boundary is shifted to the east, following at surface the trace of PTF thrust fold systems direction. The IKB strikes sub-parallel to the general trend of the seismicity and with the general attitude of the nodal planes of the focal solutions in this area, which usually correspond to N-S steep surfaces from north to south along the inner part of the Cottian Alps and to NW-SE in the southern part of Po Plain (Figure 8.2.10). Except for the focal mechanisms located near the Cavour tectonic structure, which indicate a current extensional regime, the other focal mechanisms indicate current compressional regime within the upper crust, with a direction of compression broadly perpendicular to the ENE-WSW or E-W topographic axis culmination.

Based on the good geometrical, geological, seismological, geophysical and morphological correspondence observed between IKB and the Cavour tectonic lineament and the LTZ faults systems, it seems thus that the southern segment of the IKB highlight a different crustal mobility due to a current tectonic extensional regime.

On the contrary, the northern part of the IKB does not seem to suggest a correspondence with any buried regional tectonic structure, in contrast to what argued by Perrone et al. 2011. The present crustal mobility seems instead to be consistent, at surface, with the current compressive tectonic regime of the PTF and the N–S faults bordering the inner part of the Cottian Alpine chain.

IKM reveals localized uplifting effects along the trace of NW-verging PTF complex thrust fold systems. A belt of segmented fault-propagation folds that are 10 to 40 km long and show evidence of current tectonic mobility. Structures active until Pliocene and



Pleistocene times have continued to grow later, as demonstrated by the subtle deformations induced in the Plio-Quaternary syn-growth sequence, geomorphic evidence of recent activity, geodetic levelling and the ground motion vectors revealed by GPS data (Perrone et al. 2011). In this case, the IKB can be interpreted as a “statistically-defined” boundary that separates areas with the different tectonic regime: compressive or transpressive to the west and extensive to east.

### *Sector 2*

The IKM (Figure 8.2.10) show a differential uplift and crustal mobility between the hinge line of Padan Thrust Front (PTF) between the Monferrato thrust front and Emilia thrust front, the Villalvernia-Varzi Line (VVL) and Scrivia line (SL). In the southern part of the sector 2 the IKB runs with N-S direction close to the trace of the Scrivia and Lemme tectonic lineaments and their kilometric extension under the Scrivia alluvial fan toward to the north, while in the northern part, where the PTF are masked at surface by the fluvial deposits of the eastern Po Plain, the boundary is northern-western to south-eastern, following at surface the trace of PTF thrust fold systems direction.

In particular, the N-S direction of the IKB is sub-parallel to the peculiar and narrow N-S trend seismic activity concentrated within 20 km of depth with a nodal plane of the focal solution and transpressive mechanism are in agreement with the geometry and high PS-velocity gradient observed across of this boundary (Figure 8.2.10). Field surveys allowed to verify the possible presence of a fault surface affecting the Quaternary alluvial deposits (see also references above) and their influence on the drainage network distribution.

In the northern part of sector 2, the WNW-ESE direction of the IKB marks the direction of the N-verging, buried PTF thrust and fold systems, while the IKB show a strike roughly sub-parallel to the general trend of the seismicity, which is concentrated mainly within 10 km of depth.

Therefore, as for sector 1, on the basis of the good geometrical, geological, seismological geophysical and morphological correspondence observed between IKB and the Scrivia tectonic lineaments, we can suppose that the southern part the IKB could highlight a tectonic deformation driven by a N-S steep tectonic feature associated to the Scrivia valley lineament (Figure 8.2.10). The northern part, of the IKB which has WNW-ESE direction, it is in good agreement with the present-day tectonic regime of the PTF thrust fold belt. The IKB corresponds geometrically with the strike of the thrust fold-belt systems and it shows a localized and narrow PS-velocity gradient (IKD) in agreement with the growth of a fold related to a blind thrust. Based on the kinematics and geometry of the PTF thrust and fold belt, this IKB and the IKD allow to suggest a current tectonic regime with a NE-SW shortening direction.

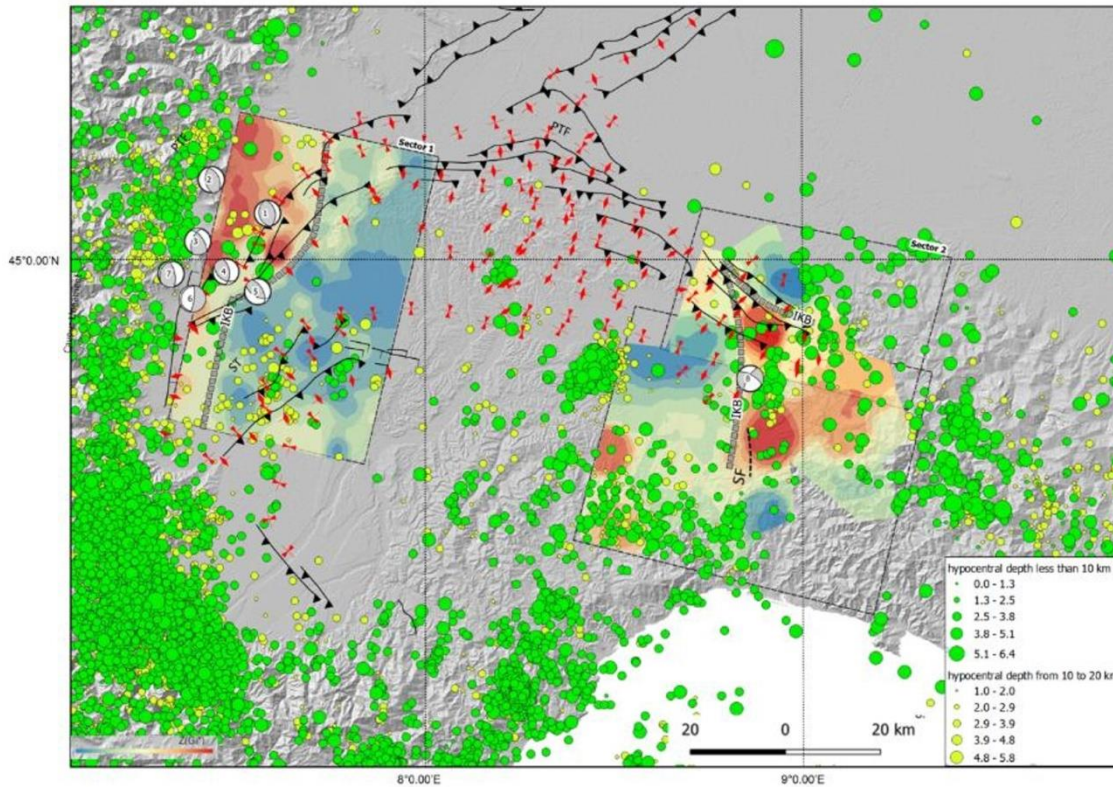


Figure 8.2.10. Map of instrumental and historical seismicity and tectonic framework of the main faults and thrust-fold-belt that includes the westernmost Po Valley. Green circles represent shallow seismicity (hypocentral depth less than 10 km) and deeper seismicity (hypocentral depth between 20 and 10 km) light green circles respectively. Focal mechanisms. Numbering corresponds to that of table 1. Iso-kinematic map and Iso-Kinematic Boundaries (IKBs) of sector 1 and sector 2. Padane Thrust Front (PTF); Scrvia Fault (SF), Savigliano Thrust (ST).



## 9 POTENTIAL IMPACT

The case studies here presented are mainly focused on the ground motion analysis and monitoring. In general, ground motion is correlated to several natural and anthropogenic phenomena such as tectonic activity, subsidence, underground fluid exploitation or storage. All these phenomena and activities have significant implications from an economic, environmental, and social point of view. In case study 1 we analyzed a portion of territory naturally affected by land subsidence because of its geographical and geological features to which the effects of anthropogenic activities are added. The Adriatic coastal area, located just south of the Po river delta, is particularly sensitive to topographical variations for the possible negative impacts on the hydrodynamic setting of the Comacchio Valleys, the hydraulic and road infrastructure, the coastline setting, the biological ecosystems, and the salinization of aquifers. The hydraulic management of the drainage channels is also involved with the relative risk of flooding, but also the challenging protection of the fragile natural habitats within the Po Delta Park and the land reclamation area, often below the current sea level.

Therefore, an efficient monitoring of ground movements and the best possible understanding of the causes that determine them are more than ever necessary for the relevant, countless and of various kinds implications that they have on our society.

Moreover, in case study 2 the IKM Iso-Kinematic Map was analyzed, based on SAR interferometry Permanent Scatterers to study the present-day crustal mobility and the differential uplift mostly driven by the activity of the major faults of a large area in western Po Plain. In particular, the relative ground movements suggested by the IKM, concentrated mainly along the IKB, could give new perspectives for interpretation of present day kinematic trends. PS-InSAR IKM methodology combined with geological and seismology knowledge can be useful to constraints on modelling earthquake source mechanisms to guide the territorial planning, industrial layouts, urban development and major infrastructure as well as public health.



## **10 IMPORTANCE OF FAULT DATABASE TO THE METHODOLOGIES APPLIED IN THE PO PLAIN CASE STUDIES**

In the procedures for the assessment of land subsidence or the definition of areas with homogeneous kinematics, object of this report, the knowledge of the tectonic component assumes primary importance. It is known that part of the regional subsidence measured in the Emilia-Romagna region has a tectonic origin (e.g. Carminati et al., 1999 and 2003b). Moreover, the geology is characterized by thrust faults and fault propagation folds related to the Apennine chain front. Therefore, the mapping and 3D modeling of faults as well as the definition of their kinematics are certainly useful for the estimation and interpretation of subsiding phenomena. The methodology, described in the case study 1, takes into consideration the tectonic component of ground deformations related to the activity of blind faults. In particular, the workflow consists of successive steps of restoration of the modeled stratigraphic surfaces, through unfolding, decompaction and unload, and removal of regional tilting and measure of the residual vertical separation along with antiformal structures, controlled by blind fault. But, to obtain an affordable estimation of the natural component of the subsidence this approach needs i) a well-constrained 3D geological model with high detail geometry of the Pleistocene-Holocene sedimentary boundaries to obtain the thickness of the units, ii) high detail 3D geometry of the thrusts, iii) the sand/shale percentage for each unit, iv) well-defined chronological constraints unit ages. This means that the only information stored in the Fault Database is necessary but not enough for the purpose. In fact, the information contained in the Fault Database should be accompanied by detailed stratigraphic information, in particular on Pleistocene-Holocene deposits. Enriching as much as possible the database with information on the 3D geometry of faulted and/or deformed stratigraphic horizons could be a possible development of the project that would allow further and wider application of the stored information.

A further target of the case studies was to define continuous velocity surface maps (Iso-Kinematic Maps: IKM) to identify regional areas characterised by homogeneous kinematics behaviour and their boundaries (Iso-Kinematic Boundaries: IKB), without focusing on PS absolute velocity values. IKB are viewed as tools to more easily verify if the PS-InSAR data on present-day crustal mobility could fit with the distribution of real tectonic structures or other geological features on the field. When IKBs correspond with a set of known geological and seismological features (faults, morpho-structural alignments, hydrographic elements, hypocentral alignments, etc.) they could be used directly to constrain a seismotectonic or regional kinematic model. In this way, the relative ground movements suggested by the IKM, concentrated mainly along the IKB, can support the interpretation of the present-day kinematic trends. Furthermore, the IKM could lead to the detection of very recent tectonic lineaments that are probably still growing at present, or also to suggest different current tectonic mobility between adjacent regions. The ground motion tendency suggested by IKM seems to be in overall agreement with the different geological and geophysical datasets. These correspondences suggest a current tectonic mobility and the differential uplift of the sectors analysed mostly driven by the activity of above major faults. Therefore on the basis of these good agreements, this methodology could also be used to associate a “weight” about the tectonic activity of faults as future expansions of the HIKE fault database.



It is remarked that the correspondence between IKB and real geological features must be seen, as regard the study cases, only in a broad statistical sense, where the boundaries separate significantly different PS velocity domains (IKD) and not in the sense of a direct correspondence with a very precisely located tectonic structure.

Although the interpretation of IKB is based on an integrated analysis of surface and subsurface geological and geophysical data, the comparison and integration with other fault data sets (e.g. the Italian Fault Database) must take into account the following limitations:

- a precise, direct correspondence between the location of faults and the IKB traces not necessarily (and not always) exists;
- the scale of field data and IKM data sets is very different;
- the knowledge of faults data in the Piemonte region, as well as the coverage of IKM data sets, is still far to be completed.



## 11 CROSS-CUTTING RELATIONS BETWEEN CASE STUDIES

The case studies apply different methodologies to the study of the potential hazards and impacts across several different kinds of energy exploitation. There are different varieties of exploitation being studied using the same methodologies, and the potential hazards and impacts for similar types of energy exploitation are being investigated using different methodologies. The following settings are investigated: a geothermal field (T3.1), decommissioned gas fields ((T3.1, T.3.4), active gas fields (T3.1, T.3.2), active oil fields (T3.1, T.3.3), and decommissioned CO<sub>2</sub> -storage (T.3.4). The applied technologies are seismology (T3.1, T3.4), InSAR-based methods (T3.2), and fault seal analysis (T3.3). All case studies have at least one cross-cutting methodology and/or exploitation type relation to another.

In addition to the energy exploitation type/hazard methodology cross-cutting relations, two overarching common themes will be explored: 1) How the different methodologies deal with uncertainties in different situations, and 2) how to improve the input to guidelines made by authorities.

### 11.1 Cross-cutting: uncertainty estimates

The methodologies being studied have different ways to deal with uncertainties, and different technologies produce uncertainties on very different spatial scales. Where surface displacement can be measured with mm precision using various InSAR-based methods, seismology works with uncertainties on epicenters of hundreds of meters and for sparse data sets of km scale. A common cross-cutting theme is: Do the uncertainties permit us to relate a specific fault to a potential hazard? In some cases inherent differences exist between the different types of data and models we would like to relate.

**In T3.2, Evaluation of methodologies for the assessment of ground deformation.** The analysis of different sets of SAR data and the calibration of InSAR data using different methodologies has revealed small, but significant differences in the estimation of subsidence. How to compare different results obtained from different types of analysis? In order to evaluate the tectonic component of subsidence, a methodology has been proposed, evidencing the intrinsic uncertainties in the assessment due to the lack of detailed information on the chronostratigraphy. Moreover, when applying PSInSAR technique to analyze tectonic mobility at a regional scale, a challenge is posed by the lack of direct correspondence between faults and isokinematic boundaries, and the significantly different scale in the data collections.

#### **IKM derived from PS-InSAR to analyse the current tectonic mobility and faults growth**

A description of a methodological approach based on statistical analysis of PS data applied to real cases of the geology of the western Po Plain, where the compatibility of the IKM with the regional geological knowledge has been tested by development of comparative methodologies (geological/geophysical and seismological data).

In particular, Hot Spot analysis is a statistical technique that enables the accurate identification of Iso-Kinematic domains (IKD) and their boundaries (IKB), without allowing the evaluation of the velocity gradient across them. To estimate these features, the ordinary kriging interpolation method of Hot Spot results was utilized. These techniques rely on the spatial correlation of HotSpot data, as inferred by variography analysis, to



determine the weighting values. These techniques have been used to define continuous velocity surface maps (here referred to as Iso-Kinematic Maps – IKM; see above for a more detailed explanation regarding the methodological approach) where Iso-Kinematic domains and Iso-Kinematic Boundaries are compared to geological/geophysical and seismological data. Iso-Kinematic domains represent land sectors characterized by homogeneous kinematic behaviour and the Iso-Kinematic Boundaries are statistical limits that bound them.

Although the geological significance of the PS-InSAR IKM and relative IKD and IKB cannot be always clearly defined, the displacement gradients that they underline surely imply a significant localization of the crustal mobility along the IKB, occurred during the time of satellite observation.

Nevertheless, irrespective of the different hypotheses applied for their interpretation, the PS-InSAR IKM can represent new constraints for geological modelling and for understanding the present-day tectonic activity. In particular, the relative ground movements suggested by the IKM, probably concentrated mainly along the IKB, could give new perspectives for interpretation of present day kinematic trends. These interpretations are not necessarily grounded on well-known, ancient geological features, but could lead to the individuation of new geological features, probably still growing at present. In this sense, the IKM could force the geologists to focus their attention on geological domains previously thought as “stable” areas, in order to develop new kinematic models, or alternatively to pose some problems as regard the suitability of PS-InSAR data for regional kinematic modelling.

## **11.2 Cross-cutting: Scientific basis for guidelines to authorities**

A common, cross-cutting goal for all of the case studies is the desire to provide improved input to authorities writing guidelines for the safe energy exploitation of the subsurface. Without proper attention and precautions, activities may lead to unwanted side effects such as earthquakes, subsidence and leakage. Guidelines based on the latest scientific findings and recognizable standards can contribute to improved safety in energy exploitation. Improved standards may also aid in the communication with the general public where safety is known to be of great interest.

In addition to the evaluation of each potential hazard in the case studies, it is relevant to consider that several different hazards may be relevant for a given energy exploitation project. For the authorities it is important to consider what is the impact of each hazard in a combined multi-hazard assessment. While HIKE may not be able to produce such a formula, the knowledge generated in the project will be made available through the Knowledge DataBase, thus highlighting the different hazards to take into account.



## 12 BEST PRACTICE WITHIN THE FIELD OF GROUND DEFORMATION ASSESSMENT METHODOLOGIES

Areal ground displacement such as land subsidence can be induced by natural phenomena but also by anthropic activities, generally with amplified effects. Underground fluid exploitation is one of the main causes of accelerated land subsidence. On the contrary, the underground storage of gas can induce ground uplifting. In Italy, the Ministry of Economic Development (MISE) in 2014 released the “Guidelines for monitoring seismicity, ground deformation and pore pressure in subsurface industrial activities” in order to define indications and guidelines for monitoring mining subsurface activities. In particular, they refer to hydrocarbon exploitation, re-injection and storage activities.

After the 2012 Emilia-Romagna (northern Italy) seismic sequence, the ICHESE Commission (International Commission on Hydrocarbon Exploration and Seismicity in the Emilia Region) highlighted the opportunity that hydrocarbons exploitation and geothermal energy production will be constantly monitored through high technology networks, with the purpose to follow the space-time evolution of microseismic activities, of ground deformations as well as of pore pressure. The Commission stated that these networks should be put into operation before new activities start, to verify and measure the background seismicity and the ground deformation behavior in non-perturbed conditions. The Commission gave a first indication about minimum networks requirements: capability to detect all the earthquakes characterized by a magnitude value of at least  $M_l$  0.5, use of satellite methods to detect ground deformations with interferometric technologies - InSAR and GNSS/GPS - with a resolution of some millimeters/year, daily bottomwell measurements of fluid pore pressure. Therefore, MiSE proceeded with the tuning of guidelines for an advanced and integrated monitoring system, finalized to the release of permissions, licenses and authorizations, and also to the surveillance on hydrocarbons exploration and exploitation and natural gas and CO<sub>2</sub> storage. The Guidelines aim at defining early observation standards for monitoring the effects of human activities, such as underground fluids reinjection (wastewaters) and hydrocarbons production/storage and, particularly, at establishing monitoring procedures and protocols, including methods to analyze the space-time evolution of some parameters representing seismicity, ground deformation and pore pressure. Before the human activities start, the monitoring allows to quantify the background values, both natural and/or induced by pre-existing human activities, of the above-mentioned parameters. During the whole operating period, the monitoring allows to distinguish and measure in continuous the possible seismicity and the variations of all the monitored parameters, compared to the background values previously acquired and estimated. In particular, seismic monitoring is intended to identify and localize the seismicity in a volume surrounding the area where human activities take place, also with the purpose to distinguish natural seismicity from the one possibly due to such activities. The monitoring must allow the space-time evolution of the seismicity to be followed with the aim, if needed, to re-modulate or interrupt (in the foreseen cases) such activities. Ground deformation monitoring is intended to identify possible surface deformation phenomena linked to the considered activities, to measure and analyze their space-time variations compared to the background conditions. By pore pressure (or reservoir) monitoring, the aim is to measure the bottom hole pressure and to carry out possible interference tests with near wells, aimed at verifying the fluid-dynamic model of that part



of subsurface interested by human activities, and at evaluating the space-time evolution of the pressures.

As regards the ground deformation monitoring features, the Guidelines indicate, for the considered survey area, a description of surface deformations detected by using InSAR measurements at least during the last 10 years, with accuracies of 5-10 mm (for what attains the single InSAR measurement in LOS) and of about 1-2 mm/year for the mean deformation velocity values. The monitoring of the ground deformation phenomena is suggested to be updated every 3 to 12 months through new InSAR measurements and for at least 3 year after the end of production, storage or underground reinjection activities. The updated InSAR measurements have to foresee the use of SAR data acquired from both ascending and descending orbits, in order to reconstruct the vertical and horizontal (E-W) components of the detected ground deformations. The InSAR measurements must be delivered with standard formats and through well established methodologies within the scientific community, for which the estimated accuracies (depending on the temporal span of the analyzed SAR image sequences and on their characteristics) have to be indicated; furthermore, the InSAR measurements have to be generated with a spatial sampling ranging between 30 and 100 m, obtained by proper spatial average operations:

The ground deformation values inferred by InSAR measurements have to be integrated/complemented with the ones provided by a continuous GPS network, already existing or newly implemented. The information obtained by the local GPS network, properly set in the international reference system (currently ITRF2008), has to allow to: make the InSAR measurements independent from the “reference zone” selected for their analysis and representation; detect (and correct) possible artifacts that can be present in InSAR measurements; perform 3D modeling of the detected deformation field. It is therefore recommended that the local GPS network foresees the placement of precision permanent stations (geodetic type), properly located depending on the size and on the characteristics of the area to be monitored. The stations have to be installed with a siting suitable for geophysical aims (e.g. UNAVCO). In particular, it is requested that the interstation distance will be less than 10-15 km with respect to the station co-located with the broad-band seismic station of the monitoring network. Finally, it is important to verify the availability of data acquired from at least 5 continuous GPS stations, operating since at least 2 years and located at less than 200-300 km far from the inner survey domain.

A planned new version of the guidelines, revised after the first period of test implementation, will overcome issues and questions that may have risen (see also Braun et al., 2021). Until now, such general indications, even if very important, leave wide margins in the choice of possible InSAR techniques and local GNSS networks to be used.

The European Environment Agency (EEA), in the framework of the implementation of the Copernicus European Ground Motion Service, has recently published on the related website (<https://land.copernicus.eu/pan-european/european-ground-motion-service>) the document “EGMS validation approach and plan”, where the requirements that GNSS data must comply with are described. According to this document, the requirements for the GNSS data include:

- The time series of the GNSS stations must have a minimum length of 3 years. Shorter time series are not reliable for the estimation of velocity (Kenyeres et al., 2019);
- The standard redistribution format constituted by the international Rinex v2.11 or v3.02 specifications is desirable;



- Accuracy and quality checks and parameters must be available for every station;
- The receiver, antenna, radome and monumentation should be consistent with the requirements defined in the EUREF Guidelines ([http://www.epncb.oma.be/\\_documentation/guidelines/](http://www.epncb.oma.be/_documentation/guidelines/)) and in the Current IGS Site Guidelines (<https://kb.igs.org/hc/en-us/articles/202011433-Current-IGS-Site-Guidelines>);
- Metadata and station logs must be available for every station and updated to the last change.

Moreover, in case different GNSS networks are available in the same area, it is recommended to make a comparison and explore any differences.

In Italy, the implementation of a Ground Motion service (designed as a Mirror Copernicus downstream service), based on interferometric data and calibrated with GNSS data, is one of the expected products of the ongoing Italian Space Economy Strategic Plan. One of the services to be implemented is the creation of a platform that collects the information (data at 30 seconds) of all the GNSS stations available at national level, also in order to define instrumental standards and guarantee the quality control of the data. Such a platform would facilitate the structuring of a reliable GNSS network, specifically dedicated to calibrating InSAR data, starting from the large number of stations already existing in Italy, which would need to be combined and harmonized.

As previously underlined the InSAR technique is often influenced by the temporal span of the analyzed SAR image sequences and on their characteristics. To solve these problems a persistent scatterer interferometry synthetic aperture radar (PSInSAR) approach (Ferretti et al., 2000 and Ferretti et al., 2001) was developed to conduct the ground deformation monitoring.

In this project, the use of PS-InSAR data has been used to assess the present-day crustal mobility that could correlate with the active faults distribution and/or tectonic mobility. To reach these goals, the PS-InSAR data has been processed with spatial statistic techniques, in order to obtain continuous PS-velocity surface maps (here referred as Iso-Kinematic Maps: IKM) that allow a better direct comparison of PS-InSAR data with the available geological maps. In this case, the comparison can be done by individuation of PS-InSAR kinematically homogeneous areas (IKD), regardless of absolute PS-velocity values, and characterization of the boundaries between them (here referred as Iso-Kinematic Boundaries: IKB). When IKB correspond with known geological features (faults, morphostructural alignments, hydrographic elements etc.) they will be used to directly constrain the seismotectonic or regional kinematic models or assess the current tectonic mobility and faults growth. In the case that the IKB do not correspond with any known geological features two possibilities exist:

- IKB could have originated by non-geological factors;
- new geological models should be envisaged to fit with PS-InSAR data;
- detection of unknown active tectonic structures.

Moreover, the use of PS-InSAR measurements for active tectonic study of areas characterized by a moderate tectonic and seismic activity, like Po Plain, must take into account the following limitations:

- the limited time of observation (1992–2001 in this case for the ERS-1/2 SAR);
- the high spatial variability of PS density;
- the PS velocity values are relative to a chosen PS reference point assumed to be stable;
- the accuracy of PS measure decreases with larger distances from the reference points;



- 
- the large distribution of negative outliers related to geomorphological or human phenomena that “mask” the shallow effect of tectonic activity;
  - the need of accurate knowledge of the geometry and kinematics of tectonic structures.



## **13 RELEVANCE OF THIS STUDY TO THE NEW GREEN DEAL AND PROPOSED FUTURE STUDIES**

In the past decade, a new generation of radar satellites have revolutionised our ability to measure Earth's surface deformation globally and with unprecedented resolution (e.g. Biggs and Wright, 2020). InSAR is transforming our understanding of ground motion and of tectonics and helping us mitigate seismic and other hazards.

Characterizing active faults and quantifying their activity are major concerns in regions with high seismic risk. Particularly in areas with a high population density and highly developed industries, these faults pose a major risk. Also subsidence is a potentially destructive hazard affecting urban and agricultural areas worldwide. Herrera et al. (2021) identified 1596 major cities, or about 22% of the world's 7343 major cities that are in potential subsidence areas, with 57% of these cities also located in floodprone areas. Moreover, subsidence threatens 15 of the 20 major coastal cities ranked with the highest flood risk worldwide. Therefore, the reduction of the uncertainties in the assessment of the ground deformation and land subsidence, focused in this report, assume a strategic importance with reference to the objectives of the European Green Deal. In fact, one of the Green Missions is the Adaptation to climate change and societal transformation. Our society will need to become resilient to sea level rise in the decades to come and low-lying coastal zones already affected by subsidence need to be given particular attention. Europe intends to become the first climate-neutral continent by 2050 and in order to achieve this goal the use of carbon capture and underground storage technologies is envisaged. In this perspective the methodologies for ground motion assessment, but also the monitoring of induced seismicity, are a key topic.

The here proposed IKM methodological approach based on PS-InSAR or InSAR data give information about the crustal tectonic mobility and the surface deformation of faults that can be useful to constraints on modelling earthquake source mechanisms to guide the territorial planning, industrial layouts, urban development and major infrastructure as well as public health.

The last decade has seen the first mission specifically designed for ground deformation monitoring (European Union's Sentinel-1 constellation), a global Digital Elevation Model with unprecedented accuracy (TanDEM-X), and a constellation of small SAR satellites capable of acquiring imagery with 1 m resolution (CosmoSkyMed). These satellites will significantly increase the potential of SAR remote sensing for ground deformation detection to better locate and quantify the activity thus to improve our knowledge of the whereabouts and mechanisms of the principal natural hazards in the different areas of Europe.



## 14 REFERENCES

- Abbate, E., Sagri, M. (1984). Le unità torbiditiche cretacee dell'appennino settentrionale ed i margini continentali della Tetide. *Memorie Società Geologica Italiana* 24, 359-375.
- Anderson, H., Jackson, J., (1987). Active tectonics of the Adriatic region. *The Geophysical Journal of the Royal Astronomical Society* 91, 937–983.
- AGIP (1972). Acque dolci sotterranee. Inventario dei dati raccolti dall'AGIP durante la ricerca di idrocarburi in Italia: pp. 914.
- AGIP (1994). Acque dolci sotterranee. Inventario dei dati raccolti dall'AGIP durante la ricerca di idrocarburi in Italia: pp. 515.
- Allievi, J., Ambrosi, C., Ceriani, M., Crosta, G. B., Ferretti, A., Fossati, D. (2003). Monitoring slow mass movements with the Permanent Scatterers Technique. *International Geosciences and Remote Sensing Symposium (IGARSS 2003)*. (pp. 1–3) Francia: Tolosa 21–25 luglio 2003.
- Amorosi A., Farina M., Severi P., Preti D., Caporale L., Di Dio G. (1996). Genetically related alluvial deposits across active fault zones: an example of alluvial fan-terrace correlation from the upper quaternary of the southern Po Basin, Italy. *Sed Geol* 102:275295.
- Antonello, G., Casagli, N., Farina, P., Leva, D., Nico, G., Sieber, A. J., et al. (2004). Ground based SAR interferometry for monitoring mass movements. *Landslides*, 1, 21–28.
- Badley M.E. (1987). *Practical seismic interpretation*. AGIP, 274 pp.
- Barbero D., Boano P., Colla M.T., Forno M.G. (2007). Pleistocene terraced succession, northern slope of Torino hill, *Quaternary International*, 171-172, 64-71.
- Berardino, P.; Fornaro, G.; Lanari, R.; Sansosti, E. (2002). A new algorithm for surface deformation monitoring based on small baseline differential SAR interferograms. *IEEE Trans. Geosci. Remote Sens.* 2002, 40, 2375–2383.
- Béthoux, N., Sue, C., Paul, A., Virieux, J., Fréchet, J., Thouvenot, F., Cattaneo, M. (2007). Local tomography and focal mechanisms in the south-western Alps: comparison of methods and tectonic implications. *Tectonophysics* 432, 1–19.
- Bigi G., Castellarin A., Coli M., Dal Piaz G.V., Sartori R., Scandone P., Vai G.B. (1990). *Structural Model of Italy scale 1:500.000, sheet 1*. C.N.R., Progetto Finalizzato Geodinamica, SELCA Firenze.
- Bitelli, G.; Bonsignore, F.; Unguendoli, M. (2000). Levelling and GPS networks to monitor ground subsidence in the Southern Po Valley. *J. Geodyn.* 2000, 30, 355–369.
- Bitelli, G.; Bonsignore, F.; Pellegrino, I.; Vittuari, L. (2015). Evolution of the techniques for subsidence monitoring at regional scale: The case of Emilia-Romagna region (Italy). *Proc. Iahs 2015*, 372, 315–321.
- Boccaletti M., Corti G., Martelli L. (2011) - A Recent and active tectonics of the external zone of the Northern Apennines (Italy). *Int J Earth Sci (GeolRundsch)* 100:1331–1348 DOI10.1007/s00531-010-0545-y
- Bondesan, M. (1985). Quadro schematico dell'evoluzione geomorfologica olocenica del territorio compreso fra Adria e Ravenna. In *Atti della tavola rotonda "Il delta del Po"*, Bologna, Italy, 24 November 1982; *Acc. Sci. dell'Ist. di Bologna*: Bologna, Italy, 1985; pp. 23–36.



- Bondesan, M. (1990). L'area deltizia padana: Caratteri geografici e geomorfologici. In *Il Parco del delta del Po: Studi ed immagini*; 21, 2 tabb; Spazio Libri Ed.: Ferrara, Italy, 1990; Volume 1, pp. 9–48.
- Boni A., Boni P., Peloso G.F., Gervasoni S. (1980). Dati sulla neotettonica del Foglio Pavia (59) e di parte dei fogli Voghera (71) ed Alessandria (70). *Pubbl. n. 356 del P.F.G. del C.N.R.*, 1199-1244.
- Bonsignore G., Bortolami, G., Elter G., Montrasio A., Petrucci F., Ragni U., Sacchi R., Sturani C. and Zanella E. (1969). Note illustrative dei Fogli 56-57, Torino-Vercelli della Carta Geologica d'Italia alla scala 1:100.000. *Serv. Geol. It., Roma*: 96 pp.
- Boschi, E., Guidoboni, E., Ferrari, G., Mariotti, D., Valensise, G., Gasperini, P. (2000). *Catalogue of Strong Italian Earthquakes*, *Ann. Geofis.* 43 (4), 268 pp.
- Braun T., Danesi S., Morelli A., (2021). Application of monitoring guidelines to induced seismicity in Italy. *J Seismol* (2020) 24:1015–1028. <https://doi.org/10.1007/s10950-019-09901-7>
- Bresciani I., Perotti C.R. (2014). An active deformation structure in the Po Plain (N Italy): the Romanengo anticline. *Tectonics*, 33. doi: 10.1002/2013TC003422.
- Bürgmann, R., Hilley, G., Ferretti, A., Novali, F. (2006). Resolving vertical tectonics in the San Francisco Bay area from GPS and permanent scatterers InSAR analysis. *Geology*, 34, 221–224.
- Calais, E., Nocquet, J.M., Jouanne, F., Tardy, M., (2002). Current strain regime in the Western Alps from continuous Global Positioning System measurements, 1996–2001. *Geology* 30, 651–654.
- Capponi, G., Crispini, L., Cortesogno, L., Gaggero, L., Firpo, M., Piccazzo, M., Cabella, R., Nosengo, S., Bonci, M.C., Vannucci, G., Piazza, M., Ramella, A., Perilli, N., et alii (2009). Note illustrative della carta geologica d'Italia alla scala 1:50.000, foglio 213-230 – Genova.
- Carraro F. (1976). Deviazione pleistocenica nel deflusso del bacino piemontese meridionale: un'ipotesi di lavoro. *Gruppo di Studio del Quaternario Padano*, 3, 89-100.
- Carminati E., Di Donato G., (1999). Separating natural and anthropogenic vertical movements in fast subsiding areas: The Po plain (N. Italy) case. *Geophys. Res. Letters*, 26, 2291–2294. doi: 10.1029/1999GL900518.
- Carminati, E.; Doglioni, C.; Scrocca, D. (2003a). Apennines subduction-related subsidence of Venice (Italy). *Geoph. Res. Lett.* 2003, 30.
- Carminati E.; Martinelli G., Severi P. (2003b). Influence of glacial cycles and tectonics on natural subsidence in the Po Plain (Northern Italy): Insights from 14C. *Geochem. Geophys. Geosyst.*, 4, 1082. doi: 10.1029/2002GC000481
- Cassano, E.; Anelli, L.; Fichera, R.; Cappelli, V. (1986). Pianura Padana: Interpretazione integrata di dati geofisici e geologici. In *Proceedings of the 73° Congresso Società Geologica Italiana*, Roma, Italy, 29 September–4 October 1986.
- Castellarin, A. (1994). Strutturazione eo-mesoalpina dell'Appennino Settentrionale attorno al "nodo ligure". In R. Capozzi & A. Castellarin (Eds.), *Studi preliminari all'acquisizione dati del profilo CROP 1-1A La Spezia - Alpi orientali*, *Studi Geologici Camerti*, Volume Speciale 1992/2, Appendice, 99–108.
- Cerrina Feroni, A., Martelli, L., Martinelli, P., Ottria, G., Catanzariti, R. (2002). *Carta Geologico-Strutturale dell'Appennino Emiliano-Romagnolo-Note Illustrative*. Regione Emilia-Romagna, Selca Firenze.
- Ciampalini A, Raspini F, Lagomarsino D, Catani F, Casagli F. (2016). Landslide susceptibility map refinement by using PSInSAR data. *Remote Sens Environ* 184:302–315.



- Colesanti, C., Ferretti, A., Ferrucci, F., Prati, C., Rocca, F. (2000). Monitoring known seismic faults using the Permanent Scatterers (PS) Technique. Proceedings of the IEEE International Geoscience and Remote Sensing Symposium, IGARSS, 24–28 July 2000, Vol. 5. (pp. 2221–2223) Honolulu (USA).
- Colesanti, C., Ferretti, A., Novali, F., Prati, C., Rocca, F. (2003a). SAR monitoring of progressive and seasonal ground deformation using the Permanent Scatterers Technique. *IEEE Transactions on Geoscience and Remote Sensing*, 41(7), 1685–1701.
- Colesanti, C., Ferretti, A., Prati, C., & Rocca, F. (2003b). Monitoring landslides and tectonic motions with the Permanent Scatterers Technique. *Engineering Geology*, 68(1), 3–14.
- Comerci, V.; Capelletti, S.; Michetti, A.M.; Rossi, S.; Serva, L.; Vittori, E. (2007). Land subsidence and Late Glacial environmental evolution of the Como urban area (Northern Italy). *Quat. Int.* 2007, 173–174, 67–86.
- Cortemiglia G.C. (2009). Segnalazione di crioturbazioni nei depositi costituenti il terrazzo “Fluviale recente” a Tortona (Piemonte – Italia) – Finding of Cryoturbations in Alluvial Terrace of “Fluviale recente” near Tortona (Piedmont Italy) Pages 75-86 © 2009 GFDQ – Geografia Fisica e Dinamica Quaternaria. Conforms to W3C Standard XHTML & CSS | 3.0.5
- Cortesogno L., Di Battistini G., Lucchetti G. & Venturelli G. (1979). Metamorphic assemblages of two high pressure-low temperature ophiolitic units of central-western Liguria: mineralogical and chemical features and tectonic significance. *Ofioliti*, 4 (2): 121-156.
- Cortesogno L., Haccard D. (1984) - Note illustrative alla carta geologica della zona Sestri-Voltaggio. *Mem. Soc. Geol. It.*, 28: 115-150.
- Crosetto, M.; Monserrat, O.; Cuevas-González, M.; Devanthery, N.; Crippa, B. Persistent Scatterer Interferometry (2016). A review. *ISPRS J. Photogr. Remote Sens.* 2016, 115, 78–89.
- Crosetto M, Solari L, Mróz M, Balasis-Levinsen J, Casagli N, Frei M, Oyen A, Moldestad DA, Bateson L, Guerrieri L, Comerci V, Andersen HS. (2020). The Evolution of Wide-Area DInSAR: From Regional and National Services to the European GroundMotion Service. *Remote Sens.*, 12, 2043; doi:10.3390/rs12122043.
- CPTI - Working Group Catalogo Parametrico dei Terremoti Italiani (2004). Catalogo Parametrico dei Terremoti Italiani, vers. 2004, Istituto Nazionale di Geofisica, Bologna, Italy.
- d’Atri A., Dela Pierre F., Festa A., Gelati R., Gnaccolini M., Piana F., Clari P., Polino R. (2002). Tettonica e sedimentazione nel “retroforeland alpino”. 81° Riunione estiva S.G.I., Torino, Guida all’escursione post-congresso, Litografia Geda, 114 pp.
- Dela Pierre, F., F. Piana, P. Boano, G. Fioraso, M.G. Forno, R. Polino, P. Clari (2003). Carta Geologica d’Italia alla scala 1:50.000, Foglio 157 “Trino”, APAT, Agenzia per la Protezione dell’Ambiente e per i Servizi Tecnici - Dipartimento Difesa del Suolo, Roma.
- Delacou, B., Sue, C., Champagnac, J.D., Burkhard, M., (2004). Present-day geodynamics in the bend of the western and central Alps as constrained by earthquake analysis. *Geophys. J. Int.* 158, 753-774.
- Delacou, B., Sue, C., Nocquet, J.M., Champagnac, J.D., Allanic, C., Burkhard, M. (2008). Quantification of strain rate in the Western Alps using geodesy: comparisons with seismotectonics. *Swiss J Geosci* 101, 377-385.



- Delacou, B., Sue, C., Nocquet, J.M., Champagnac, J.D., Allanic, C., Burkhard, M., 2008. Quantification of strain rate in the Western Alps using geodesy: comparisons with seismotectonics. *Swiss J Geosci* 101, 377-385.
- Devoti R., Esposito A., Pietrantonio G., Pisani A. R., Riguzzi F. (2011). Evidence of large-scale deformation patterns from GPS data in the Italian subduction boundary. *Earth and Planetary Science Letters* 311 (2011) 230–241.
- Dialuce, C. Chiarabba, D. Di Bucci, C. Doglioni, P. Gasparini, R. Lanari, E. Priolo, A. Zollo, (2014). Guidelines for monitoring seismicity, ground deformation and pore pressure in subsurface industrial activities. Available online: [https://unmig.mise.gov.it/images/docs/151\\_238.pdf](https://unmig.mise.gov.it/images/docs/151_238.pdf)
- Di Giulio, A., Galbiati, B. (1995). Interaction between tectonics and deposition into an episutural basin in the Alps-Appennines knot. In R. Polino & R. Sacchi (Eds.), *Atti del Convegno sul tema 'Rapporti tra Alpi e Appennino' e guida alle escursioni* (pp. 113–128). Roma: Accademia Nazionale delle Scienze detta dei XL, Scritti e Documenti.
- Di Giulio A., Carrapa B., Fantoni R., Gorla L., Valdistrullo A. (2001). Middle Eocene to Early Miocene sedimentary evolution of the western Lombardian segment of the South Alpine foredeep (Italy), *Int. J. Earth Sciences (Geol. Rundsch)*, 90: 534-548.
- Durand-Riard P., Salles L., Ford M., Caumon G. & Pellerin J. (2011). Understanding the evolution of syn-depositional folds: Coupling decompaction and 3D sequential restoration. *Marine Petr. Geol.*, 28 (8), 1530-1539.
- EEA and Copernicus. Available online: <https://www.eea.europa.eu/aboutus/who/copernicus-1>
- Ellero, A. (2000). Assetto strutturale delle Unità Liguri Interne della Val Polcevera e dell'alta valle Scrivia (Appennino Settentrionale). *Bollettino Società Geologica Italiana*, 119,321-338.
- Elter P., Pertusati P. (1973) – Considerazioni sul limite Alpi-Appennino e sulle sue relazioni con l'arco delle Alpi occidentali. *Mem. Soc. Geol. It.*,12, 359-375.
- ENEL (1981) - Elementi di neotettonica del territorio italiano. 95 pp.
- Eni S.p.A. (2015) Appendice C—Studio e Piano di Monitoraggio Subsidenza. In Studio di impatto ambientale. Istanza di Concessione di Coltivazione Agosta. Messa in produzione del pozzo Agosta 1 Dir. Giugno 2015. SICS-210-APP-C. Available online: <http://www.va.minambiente.it/it-IT/Oggetti/Documentazione/1552/2515?Testo=Appendice+C+%E2%80%93+Studio+e+Piano+di+Monitoraggio+Subsidenza.&RaggruppamentoID=&x=17&y=14#formcercaDocumentazione> (accessed on 15 April 2021).
- Eni S.p.A. (2016) Allegato 6b. Analisi Geodinamica campo di Dosso degli Angeli e Agosta. In *Integrazioni allo Studio di Impatto Ambientale*. Luglio 2016. Available online: <http://www.va.minambiente.it/it-IT/Oggetti/Documentazione/1552/2515?Testo=geodinamica&RaggruppamentoID=&x=11&y=12#formcercaDocumentazione> (accessed on 15 April 2021).
- Eni S.p.A. (2016b). Allegato 11. Relazione tecnica Geologia, Geotecnica e Sismica. Luglio 2016. *Integrazioni allo studio di impatto ambientale*. SICS\_210\_Integraz. Progetto messa in produzione pozzo Agosta 1 Dir. Available online: <https://va.minambiente.it/it-IT/Oggetti/Documentazione/1552/2515?Testo=geodinamica&x=11&y=12&pagina=5> (accessed on 18 April 2021).
- Eva, C., Augliera, P., Cattaneo, M., Pastore, S., Tomaselli, A. (1990). Revisione di dati sismometrici in Italia Nord-Occidentale nel periodo 1971-1989. *Atti del Convegno Gruppo Nazionale Difesa dai terremoti*, Ed. Ambiente - Pisa 1, 25-34.



- Eva E., Solarino S. (1992). Alcune Considerazioni sulla Sismotettonica dell'Appennino Nord-Occidentale Ricavate dall'analisi dei Meccanismi Focali. Studi Geol. Camerti, Vol. Spec. 2, Append. Crop 1-1a, 75-83.
- Eva, E., Solarino, S. (1998). Variation of stress directions in the western Alpine arc, Geophys. J. Int. 135, 438-448.
- Eva, E., Solarino, S., Eva, C., Neri, G. (1997). Stress tensor orientation derived from fault plane solution in the Southwestern Alps. J Geophys Res 102, 8171-8185.
- EUREF Permanent GNSS Network. Available online: <http://epncb.eu/>
- Fantoni, R.; Franciosi, R. (2010). Tectono-sedimentary setting of the Po Plain and Adriatic Foreland. Rend. Lincei-Sci. Fis. Nat. 2010, 21, 197–209.
- Farina, P., Colombo, D., Fumagalli, A., Marks, F., & Moretti, S. (2006). Permanent Scatterers for landslide investigations: Outcomes from the ESA-SLAM project. Engineering Geology, 88, 200–217.
- Farolfi, G.; Maseroli, R.; Baroni, L.; Cauli, F. Final results of the Italian “Rete Dinamica Nazionale” (RDN) of Istituto Geografico Militare Italiano (IGMI) and its alignment to ETRF2000. In Proceedings of the Symposium EUREF 2009, Firenze, Italy, 27–29 May 2009.
- Felletti, F., (2004). Statistical modelling and validation of correlation in turbidites: an example from the Tertiary Piedmont Basin (Castangola Fm., Northern Italy). Marine and Petroleum Geology, 21, 23-39
- Ferretti, A.; Prati, C.; Rocca, F. (2000). Nonlinear subsidence rate estimation using permanent scatterers in differential SAR interferometry. IEEE Trans. Geosci. Remote Sens. 2000, 38, 2202–2212.
- Ferretti, A.; Prati, C.; Rocca, F. (2001). Permanent scatterers in SAR interferometry. IEEE Trans. Geosci. Remote Sens. 2001, 39, 8–20.
- Ferretti, A., Prati, C., Rocca, F., Casagli, N., Farina, P., Young, B. (2005). Permanent Scatterers Technology: a powerful state of the art tool for historic and future monitoring of landslides and other terrain instability phenomena. Proceeding International Landslide Symposium - ISL2005 Vancouver (Canada).
- Festa, A., Dela Pierre, F., Irace, A., Piana, F., Fioraso, G., Lucchesi, S., Boano, P., and Forno, M.G., (2009). Note illustrative della Carta Geologica d'Italia, scale 1:50.000, 156 sheet - Torino Est: ISPRA – Rome, Italy, 143 p.
- Festa, A., Fioraso, G., Bissacca, E., Petrizzo, M.R. (2015). Geology of the Villalvernia–Varzi Line between Scrivia and Curone valleys (NW Italy). Journal of Maps 11 (1), 39–55.
- Fiaschi, S.; Tessitore, S.; Bonì, R.; Di Martire, D.; Achilli, V.; Borgstrom, S.; Ibrahim, A.; Floris, M.; Meisina, C.; Ramondini, M.; et al. (2016). From ERS-1/2 to Sentinel-1: Two decades of subsidence monitored through A-DInSAR techniques in the Ravenna area (Italy). Giscience Rem. Sens. 2016.
- Forno M. G. (1982) - Studio geologico dell'Altopiano di Poirino (Torino). Geogr. Fis. Dinam. Quat., 5, 129-162.
- Fossati A., Perotti C., Vercesi P. L. (1988). Deformazioni tettoniche al margine sud-orientale del bacino terziario ligure-piemontese. Rend. Soc. Geol. It .11, f.2: 305-308, Roma
- Funning, G. J., Bürgmann, R., Ferretti, A., Novali, F., Fumagalli, A. (2007). Creep on the Rodgers Creek fault, northern San Francisco Bay area from a 10 year PS-InSAR dataset. Geophysical Research Letters, 34, L19306.



- Gambolati, G.; Teatini, P.; Ferronato, M. (2006). Anthropogenic Land Subsidence. In Encyclopedia of Hydrological Sciences; Anderson, M.G., McDonnell, J.J., Eds.; Wiley: Hoboken, NJ, USA, 2006.
- Gelati, R. (1977). La successione eo-oligocenica di Garbagna (Alessandria) al margine orientale del Bacino Terziario Ligure Piemontese. *Rivista Italiana di Paleontologia*, 83, 103-136.
- Gelati, R., Gnaccolini, M., (1988). Sequenze deposizionali in un bacino episaturale, nella zona di raccordo tra Alpi e Appennino settentrionale. *Atti Ticinensi di Scienze della Terra* 31, 340–350.
- Gelati R., Napolitano A., Valdistorlo A. (1988), La 'Gonfolite Lombarda': stratigrafia e significato nell'evoluzione del margine sudalpino, *Riv. Ital. Paleontol. Strat.*, 94(2): 285-332.
- Gelati R., Gnaccolini M., Polino R., Mosca P., Piana F., Morelli M., Fioraso G. (2010). Note illustrative della Carta Geologica d'Italia alla scala 1:50.000. Foglio 211 "Dego". ISPRA - Istituto Superiore per la Protezione e la Ricerca Ambientale, Roma, 124 pp.
- GeoMol Team (2015). GeoMol – Assessing subsurface potentials of the Alpine Foreland Basins for sustainable planning and use of natural resources – Project Report, 188 pp. (Augsburg, LfU). [www.geomol.eu/report/index\\_html](http://www.geomol.eu/report/index_html) [2020-11-12]
- Getis, A., Ord, J.K., (1992). The analysis of spatial association by use of distance statistics. *Geographical Analysis* 24 (3), 189–206.
- Ghibaudo, G., Clari, P., Perello, M. (1985). Litostratigrafia, sedimentologia ed evoluzione tettonico sedimentaria dei depositi miocenici del margine sud-orientale del Bacino terziario Ligure - Piemontese. *Bollettino della Società Geologica Italiana*, 104, 349-397.
- Ghielmi M., Vigna B., Violanti D., Rogledi S., Amore M.R., (2002). Evoluzione tettono-sedimentaria della successione plio-pleistocenica nel settore del Piemonte centro-meridionale. *Atti 81a Riunione estiva della Società Geologica Italiana*, Torino, 10-12 settembre 2002, 181-182
- Ghielmi M, Rogledi S., Vigna B., Violanti D. (2019). La successione Messiniana e Plio-Pleistocenica del Bacino di Savigliano (Settore Occidentale del Bacino Terziario Piemontese) *Geol. Insubr.* 13/1 ISSN 1420-9500.
- Gutierrez M. & Wangen M. (2005). Modeling of compaction and overpressuring in sedimentary basins. *Marine and Petroleum Geology*, 22, 351-363.
- Herrera-García G., Ezquerro P., Tomás R., Béjar-Pizarro M., López-Vinielles J., Rossi M., Mateos R.M., Carreón-Freyre D., Lambert J., Teatini P., Cabral-Cano E., Erkens G., Galloway D., Hung W., Kakar N., Sneed M., Tosi L., Wang H., Ye S. (2021). Mapping the global threat of land subsidence. *Science*. Vol 371 Issue 6524. [sciencemag.org](http://sciencemag.org)
- Herrera, G., Davalillo, J. C., Mulas, J., Cooksley, G., Monserrat, O., & Pancioli, V. (2009). Mapping and monitoring geomorphological processes in mountainous areas using PSI data: Central Pyrenees case study. *Natural Hazards and Earth System Sciences*, 9, 1587–1598.
- Hilley, G. E., Burgmann, R., Ferretti, A., Novali, F., & Rocca, F. (2004). Dynamics of slow moving landslides from Permanent Scatterers analysis. *Science*, 304(5679), 1952–1955.
- Hoogerduijn Strating E.H. (1994). Extensional faulting in an intraoceanic subduction complex - working hypothesis for the Paleogene of the Alps-Appennine system. *Tectonophysics*, 238: 255-273



- INGV (2007). Catalogo dei terremoti recenti in Italia. [www.ingv.it](http://www.ingv.it)
- InSAR Norway. Available online: <https://www.ngu.no/en/topic/insar-norway>
- International Commission on Hydrocarbon Exploration and Seismicity in the Emilia Region; [http://mappegis.regione.emiliaromagna.it/gstatico/documenti/ICHESE/ICHESE\\_Report.pdf](http://mappegis.regione.emiliaromagna.it/gstatico/documenti/ICHESE/ICHESE_Report.pdf)
- Kenyeres, A., Bellet, J. G., Bruyninx, C., Caporali, A., de Doncker, F., Droscak, B. et al. (2019). Regional integration of long-term national dense GNSS network solutions. *GPS Solutions*, 23(4), 122.
- Lanari, R.; Casu, F.; Manzo, M.; Zeni, G.; Bernardino, P.; Manunta, M.; Pepe, A. (2007). An overview of the small baseline subset algorithm: A DInSAR technique for surface deformation analysis. *Pure Appl. Geophys.* 2007, 164, 637–661.
- Laubscher P., Biellag C., Assinris C., Gelatri ., Lozeaj ., Scarascia., Tabacco (1992). The collisional knot in Liguria. *Geologische Rundschau*, 8112, 275-289.
- Levi, N., Ellero, A., Pandolfi, L., Ottria, G. (2006). Polyorogenic deformation history recognized at shallow structural levels: the case of the Antola unit (Northern Apennine, Italy). *Journal of Structural Geology* 28, 1694-1709.
- Maesano F.E., Toscani G., Burrato P., Mirabella F., D'ambrogi C., Basili R. (2013). Deriving thrust fault slip rates from geological modeling: examples from the Marche coastal and offshore contraction belt, Northern Apennines, Italy. *Marine Petr. Geol.*, 42, 122-134. doi: 10.1016/j.marpetgeo.2012.10.008.
- Maesano F.E. & D'Ambrogi C. (2016). Coupling sedimentation and tectonic control: Pleistocene evolution of the central Po Basin. *It. J. Geosci.*, 135(3), 394-407. doi: 10.3301/IJG.2015.17.
- Martelli, L.; Bonini, M.; Calabrese, L.; Corti, G.; Ercolessi, G.; Molinari, F.C.; Piccardi, L.; Pondrelli, S.; Sani, F.; Severi, P. (2017). Note Illustrative della Carta Sismotettonica della Regione Emilia Romagna ed aree limitrofe. In *Carta sismotettonica della Regione Emilia-Romagna e aree limitrofe; Regione Emilia Romagna, Ed.; DREAM: Pratovecchio Stia (AR), Italy, 2017; p. 94. Available online: [http://mappegis.regione.emilia-romagna.it/gstatico/documenti/sismotett\\_2016/Nota\\_Illustrativa.pdf](http://mappegis.regione.emilia-romagna.it/gstatico/documenti/sismotett_2016/Nota_Illustrativa.pdf) (accessed on 27 March 2021).*
- Maseroli, R. (2015). Evoluzione del Sistema Geodetico di Riferimento in Italia: La RDN2. *Boll. Ass. It. Cart.* 2015, 153, 19–44.
- Massa, M., Eva, E., Spallarossa, D., Eva, C., (2006). Detection of earthquake clusters on the basis of waveform similarity: an application in the Monferrato Region (Piedmont, Italy), *J. Seismol.*, 10, 1–22.
- Massironi, M., Zampieri, D., Bianchi, M., Schiavo, A., Franceschini, A. (2009). Use of PSInSAR (TM) data to infer active tectonics: Clues on the differential uplift across the Giudicarie belt (Central-Eastern Alps, Italy). *Tectonophysics*, 476(1–2), 297–303.
- MATTM Environmental Assessments and Authorizations. Available online: <http://www.va.minambiente.it/en-GB/Oggetti/Info/1552>
- Meisina, C. (2003). Light buildings on swelling/shrinking soils: case histories from Oltrepo Pavese (north-western Italy). *Int. Conf. on Problematic Soils, Nottingham, July 28-30, 2*, 365-374.
- Michetti, A.M., Giardina, F., Livio, F., Mueller, K., Serva, L., Sileo, G., Vittori, E., Devoti, R., Riguzzi, F., Carcano, C., Rogledi, S., Bonadeo, L., Brunamonte, F., Fioraso, G. (2012). Active compressional tectonics, Quaternary capable faults and the seismic landscape of the Po Plain (N Italy). *Ann. Geophys.* 55 (5), 969–1001.



- Mitchum R.M., Vail P.R., Sangree J.B. (1977). Seismic stratigraphy and global changes of sea level, part 7: stratigraphic interpretation of seismic reflection patterns in depositional sequences. In: Seismic stratigraphy – Applications to Hydrocarbon Exploration. Mem. Am. Ass. petr. Geol., 26, 135-144.
- Morelli, M., Piana, F., Fioraso, G., Mallen, L., Nicolò, G. (2008). Analysis of interferometry data (permanent scatterers: PS-InSAR) to identify active tectonic structures in Western Alps (NW Italy). American Geophysical Union, Fall Meeting, December 2008 San Francisco (CA).
- Morelli, M., Piana, F., Mallen, L., Nicolò, G., Fioraso, G. (2011). Iso-Kinematic Maps from statistical analysis of PS-InSAR data of Piemonte, NW Italy: comparison with geological kinematic trends. Remote Sensing of Environment 115, 1188–1201.
- Mosca P., Polino R., Rogledi S. & Rossi M. (2010). New data for the kinematic interpretation of the Alps-Appennines junction (Northwestern Italy). Int. J. Earth Sci., 99: 833-849.
- Mutti, E., Papani, L., Di Biase, D., Davoli, D., Mora, S., Segadelli, S., Tinterri, R. (1995). Il Bacino Terziario Epimesoalpino e le sue implicazioni sui rapporti tra Alpi ed Appennino. Memorie di Scienze Geologiche di Padova, 47, 217-244.
- Nicolas, M., Santoire, J.P., Delpech, P.Y., (1990). Intraplate seismicity: new seismotectonic data in Western Europe. Tectonophysics 179, 27-53.
- Notti D, Herrera G, Bianchini S, Meisina C, García-Davalillo JC, Zucca F (2014). A methodology for improving landslide PSI data analysis. Int J Remote Sens 35(6):2186–2214
- Ord, J.K., Getis, A. (1995). Local spatial autocorrelation statistics. Geographical Analysis 4 (27), 286–306.
- Perotti C.R. (1995). Analisi strutturale dei depositi conglomeratici neogenici affioranti lungo il margine padano dell'Appennino pavese-piacentino. Atti Tic. Sc. Terra, Serie Spec. 3: 89-98. Pavia, 1995.
- Perrone, G., Eva, E., Solarino, S., Cadoppi, P., Balestro, G., Fioraso, G., Tallone, S., (2010). Seismotectonic investigations in the inner Cottian Alps: an integrated approach. Tectonophysics 496, 1-16.
- Perrone, G., Cadoppi, P., Balestro, G., Tallone, S., (2011). Post-collisional tectonics in the Northern Cottian Alps (Italian Western Alps). Int. J. Earth Sciences 100, 1349–1373.
- Perrone G., Morelli M., Piana F., Fioraso G., Nicolò G., Mallen G., Cadoppi P., Balestro G., Tallone S. (2013). Current tectonic activity and differential uplift along the Cottian Alps/Po Plain boundary (NW Italy) as derived by PS-InSAR data. Journal of Geodynamics, 66, 65-78.
- Piana, F. (2000). Structural features of western Monferrato (Alps-Appennines junction zone, NW Italy). Tectonics 19, 943-960.
- Piana F., Fioraso G., Irace A., Mosca P., d'Atri A., Barale L., Falletti P., Monegato G., Morelli M., Tallone S., Vigna G.B. (2017a). Geology of Piemonte Region (NW Italy, Alps-Appennines junction zone). Journal of Maps, 13,2, 395-405.
- Piana F., Barale L., Compagnoni R., d'Atri A., Fioraso G., Irace A., Mosca P., Tallone S., Monegato G., Morelli M. (2017b). Geological Map of Piemonte Region at 1:250,000 scale Explanatory Notes. Acc. Sc. Torino Memorie Sc. Fis. 41 (2017), 3-143, 1 tab., 16 figg.
- Picotti V., Capozzi R., Bertozzi G., Mosca F., Sitta A., Tornaghi M. (2007). The Miocene petroleum system of the Northern Apennines in the central Po Plain (Italy). In: Lacombe O., Roure F., Lavé J. & Vergés J. (eds.), Thrust Belts and Foreland Basins,



- From Fold Kinematics to Hydrocarbon System. SE-25, *Frontiers in Earth Sciences*. Springer Berlin Heidelberg, 117-131.
- Pieri, M.; Groppi, G., 1981. Subsurface Geological Structure of the Po Plain. Progetto Finalizzato Geodinamica, Agip (414), pp. 23.
- Regione Emilia Romagna, ARPAE. Progetto integrato per la tutela dell'acquifero, la lotta alla subsidenza e alla erosione costiera. Studio della subsidenza tramite interferometria. Bologna, maggio 2003. Available online: [https://www.arpae.it/cms3/documenti/subsidenza/Rel\\_autbacmarecchi](https://www.arpae.it/cms3/documenti/subsidenza/Rel_autbacmarecchi).
- Regione Emilia Romagna, ARPAE. Rilievo della subsidenza nella Pianura Emiliano-Romagnola. Analisi Interferometrica. Bologna, maggio 2007. Available online: <https://ambiente.regione.emilia-romagna.it/it/acque/approfondimenti/documenti/rilievo-della-subsidenza-nella-pianura-emilianoromagnola>
- Regione Emilia Romagna, ARPAE. Rilievo della subsidenza nella Pianura Emiliano-Romagnola. Relazione Finale. Bologna, ottobre 2012. Available online: [https://www.google.com.hk/url?sa=t&rct=j&q=&esrc=s&source=web&cd=1&ved=2ahUKewilqJ7Ss5\\_iAhW5KqYKHAM3C2MQFjAAegQIBBAB&url=https%3A%2F%2Fwww.arpae.it%2Fcms3%2Fdocumenti%2Fsubsidenza%2FRelfin\\_2012.pdf&usq=AOvVaw1J3MerGansNDGDRd5DiCyp](https://www.google.com.hk/url?sa=t&rct=j&q=&esrc=s&source=web&cd=1&ved=2ahUKewilqJ7Ss5_iAhW5KqYKHAM3C2MQFjAAegQIBBAB&url=https%3A%2F%2Fwww.arpae.it%2Fcms3%2Fdocumenti%2Fsubsidenza%2FRelfin_2012.pdf&usq=AOvVaw1J3MerGansNDGDRd5DiCyp)
- Regione Emilia Romagna, ARPA Ingegneria Ambientale. Misura della rete regionale di controllo della subsidenza, misura di linee della rete costiera non comprese nella rete regionale, rilievi batimetrici. Relazione finale. Bologna, ottobre 2001. Available online: [https://www.arpae.it/cms3/documenti/subsidenza/Relfin\\_2001.PDF](https://www.arpae.it/cms3/documenti/subsidenza/Relfin_2001.PDF)
- Regione Emilia Romagna, ARPAE. Rilievo della subsidenza nella Pianura Emiliano-Romagnola. Seconda fase. Relazione finale. Bologna, aprile 2018. Available online: [https://www.google.com.hk/url?sa=t&rct=j&q=&esrc=s&source=web&cd=1&ved=2ahUKewiT192PtJ\\_iAhXKwosBHa86A6MQFjAAegQIAhAB&url=https%3A%2F%2Fambiente.regione.emiliaromagna.it%2Fit%2Facque%2Fapprofondimenti%2Fdocumenti%2Frilievo-della-subsidenza-nella-pianura-emilianoromagnola%2Fseconda-fase&usq=AOvVaw2J83kjuul74JEdFMDikbFt](https://www.google.com.hk/url?sa=t&rct=j&q=&esrc=s&source=web&cd=1&ved=2ahUKewiT192PtJ_iAhXKwosBHa86A6MQFjAAegQIAhAB&url=https%3A%2F%2Fambiente.regione.emiliaromagna.it%2Fit%2Facque%2Fapprofondimenti%2Fdocumenti%2Frilievo-della-subsidenza-nella-pianura-emilianoromagnola%2Fseconda-fase&usq=AOvVaw2J83kjuul74JEdFMDikbFt)
- Regione Emilia Romagna. Delibera di Giunta Regionale n. 539 del 28/04/2017. Procedura di VIA Ministeriale-Parere in merito alla valutazione di impatto ambientale dell'istanza di concessione di coltivazione Agosta-messa in produzione del pozzo Agosta 1 dir" nel Comune di Comacchio (art. 25, comma 2 del D.lgs. 152/06). Bologna, Italy, 2017. Available online: <http://www.va.minambiente.it/it-IT/Oggetti/Documentazione/1552/2515?Testo=66.67.%09Regione+Emilia+Romagna.+Delibera+di+Giunta+Regionale+n.+539+del+28%2F04%2F2017&RaggruppamentoID=&x=19&y=14#form-cercaDocumentazione>
- Rossi, M., Mosca, P., Polino, R., Rogledi, S., Biffi, U, (2009). New outcrop and subsurface data in the Tertiary Piedmont Basin (NW- Italy): unconformity-bounded stratigraphic units and their relationships with basin-modification phases. *Riv. Ital. Paleont. Strat.* 3, 305-335.
- Rossi M., Minervini M., Ghielmi M. & Rogledi S. (2015). Messinian and Pliocene erosional surfaces in the Po Plain-Adriatic Basin: Insights from allostratigraphy and sequence stratigraphy in assessing play concepts related to accommodation and gateway turnarounds in tectonically active margins. *Mar. Pet. Geol.*, 66, 192-216. doi: 10.1016/j.marpetgeo.2014.12.012.
- Rothé, J.P. (1941). Les séismes des Alpes françaises en 1938 et la sismicité des Alpes occidentales, *Annales de l'Institut de Physique du Globe Strasbourg*, 3, 1-105.



- Scholle, P.A. (1970) - The Sestri-Voltaggio Line: a transform fault induced tectonic boundary between the Alps and the Apennines. *American Journal of Science*, 269, 343-359.
- Schumacher, M. E., Laubscher, H. P. (1996). 3D crustal architecture of the Alps–Apennines join – a new view on seismic data. *Tectonophysics*, 260, 349–363.
- Slater J.G., Christie P.A.F. (1980). Continental stretching: an explanation of the post-Mid-Cretaceous subsidence of the Central North Sea Basin. *Journal of Geophysical Research*, 85 (B7), 3711-3739.
- Scrocca D., Carminati E., Doglioni C. & Marcantoni D. (2007). Slab Retreat and Active Shortening along the Central-Northern Apennines. In: Lacombe O., Roure F., Lavé J. & Vergés J. (eds.), *Thrust Belts and Foreland Basins. SE-25, Frontiers in Earth Sciences*. Springer Berlin Heidelberg, 471-487. doi: 10.1007/978-3-540-69426-7\_25.
- Simeoni, U.; Tessari, U.; Corbau, C.; Tosatto, O.; Polo, P.; Teatini, P. (2017). Impact of land subsidence due to residual gas production on surficial infrastructures: The Dosso degli Angeli field study (Ravenna, Northern Italy). *Eng. Geol.* 2017, 229.
- Sturani, C. (1973). Considerazioni sui rapporti tra Appennino Settentrionale ed Alpi Occidentali. Estratto dal quaderno n. 183. *Atti del Convegno sul tema: "Moderne vedute sulla geologia dell'Appennino"*, 183, 119-142.
- Sue, C., Thouvenot, F., Frechét, J., Tricart, P. (1999). Widespread extension in the core of the western Alps revealed by earthquake analysis. *J Geoph Res* 104, 25611-25622.
- Sue, C., Tricart, P. (2003). Neogene to current normal faulting in the inner western Alps: A major evolution of the late alpine tectonics. *Tectonics* 22(5):1050, doi:10.1029/2002TC001426, 2003.
- Sue, C., Delacou, B., Champagnac, J.D., Allanic, C., Tricart, P., Burkhard, M. (2007). Extensional neotectonics around the bend of the Western/Central Alps: an overview. *Int J Earth Sci* 96, 1101-1129.
- Teatini, P.; Tosi, L.; Strozzi, T. (2011). Quantitative evidence that compaction of Holocene sediments drives the present land subsidence of the Po Delta, Italy. *J. Geophys. Res.* 2011, 116, B08407.
- Tomaselli A., Pastore S., Augliera P., Eva C. (1992). Sismicità dell'Appennino nord-occidentale. In: *Studi Geologici Camerti, Vol. Speciale 1992-2, CROP 1-1A*, pp. 43-50.
- Tosi, L.; Teatini, P.; Strozzi, T. (2013). Natural versus anthropogenic subsidence of Venice. *Sci. Rep.* 2013, 3, 2710
- Vigna B., Fiorucci A., Ghielmi M. (2010). Relations between stratigraphy, groundwater flow and hydrogeochemistry in Poirino Plateau and Roero areas of the Tertiary Piedmont Basin – Italy. *Mem. Descr. Carta Geol. d'It.*, XC, 267-292.
- Vitagliano E., Riccardi U., Piegari E., Boy J.P., Di Maio R. (2020). Multi-Component and Multi-Source Approach for Studying Land Subsidence in Deltas. *Remote Sensing*, 12, 1465. doi: 10.3390/rs12091465.
- Ward, S. (1994). Constraints on the seismotectonics of the central Mediterranean from very long baseline interferometry. *Geophysical Journal International* 117, 441–452.
- Wilson L.F., Pazzaglia F.J., Anastasio D.J. (2009). A fluvial record of active fault-propagation folding, Salsomaggiore anticline, northern Apennines, Italy. *J. Geophys. Res.*, 114, B08403. doi: 10.1029/2008JB005984.



---

## **15 SUPPLEMENTARY MATERIAL**

### **15.1 Guidelines for monitoring seismicity, ground deformation and pore pressures in subsurface industrial activities (Italy)**

The guidelines, published in 2014 by the Ministry of Economic Development (MiSE), refer to a first experimental phase on pilot fields representative of the various cases concerning oil production with water reinjection, natural gas storage and geothermal production. The document defines the characteristics of the monitoring networks to be created and the performances they must guarantee. The document represents the general guidelines and criteria for the formulation of good practices, to be applied to the individual concessions according to the characteristics of the site and the characteristics of the reinjection, extraction or storage project.

By: G. Dialuce, C. Chiarabba, D. Di Bucci, C. Doglioni, P. Gasparini, R. Lanari, E. Priolo, A. Zollo, (2014) for the Ministry of Economic Development (MiSE).

### **15.2 The need for a standardized methodology for quantitative assessment of natural and anthropogenic land subsidence: The Agosta (Italy) Gas Field case**

A paper demonstrating the need for a standardized methodology for ground deformation assessment and GNSS calibration of InSAR data.

By: V. Comeci & E. Vittori (2019), in: Remote Sensing, 11, 1178;  
doi:10.3390/rs11101178